The EMBO Journal (2007) 26, 3283–3295 | © 2007 European Molecular Biology Organization | All Rights Reserved 0261-4189/07
www.embojournal.org

THE EMBO JOURNAL

Latent TGF-β-binding protein 2 binds to DANCE/fibulin-5 and regulates elastic fiber assembly

Maretoshi Hirai[1,2,5], Masahito Horiguchi[1,2,5], Tetsuya Ohbayashi[1], Toru Kita[2], Kenneth R Chien[3] and Tomoyuki Nakamura[1,4,*]

[1]Horizontal Medical Research Organization, Graduate School of Medicine, Kyoto University, Kyoto, Japan, [2]Department of Cardiovascular Medicine, Graduate School of Medicine, Kyoto University, Kyoto, Japan, [3]Cardiovascular Research Center, Massachusetts General Hospital, Harvard Medical School, Charlestown, MA, USA and [4]Department of Pharmacology, Kansai Medical University, Osaka, Japan

Elastic fibers play the principal roles in providing elasticity and integrity to various types of human organs, such as the arteries, lung, and skin. However, the molecular mechanism of elastic fiber assembly that leads to deposition and crosslinking of elastin along microfibrils remains largely unknown. We have previously shown that developing arteries and neural crest EGF-like protein (DANCE) (also designated fibulin-5) is essential for elastogenesis by studying DANCE-deficient mice. Here, we report the identification of latent transforming growth factor-β-binding protein 2 (LTBP-2), an elastic fiber-associating protein whose function in elastogenesis is not clear, as a DANCE-binding protein. Elastogenesis assays using human skin fibroblasts reveal that fibrillar deposition of DANCE and elastin is largely dependent on fibrillin-1 microfibrils. However, downregulation of LTBP-2 induces fibrillin-1-independent fibrillar deposition of DANCE and elastin. Moreover, recombinant LTBP-2 promotes deposition of DANCE onto fibrillin-1 microfibrils. These results suggest a novel regulatory mechanism of elastic fiber assembly in which LTBP-2 regulates targeting of DANCE on suitable microfibrils to form elastic fibers.

The EMBO Journal (2007) **26,** 3283–3295. doi:10.1038/sj.emboj.7601768; Published online 21 June 2007
Subject Categories: cell & tissue architecture
Keywords: DANCE; elastic fiber; fibulin-5; LTBP-2; microfibril

Introduction

Elastic matrices impart resilience and structural integrity to various types of human organs, such as the large arteries, lungs, and skin (Rosenbloom *et al*, 1993). They play especially vital roles in the functions of the arteries and lungs, which undergo repeated cycles of extension and recoil to maintain the blood pressure or breathing process. Injury and degeneration of elastic matrices are profoundly associated with age-related symptoms and diseases, such as arteriosclerosis, lung emphysema, and wrinkled skin (Pasquali-Ronchetti and Baccarani-Contri, 1997; Bailey, 2001). Elucidating the mechanisms of elastogenesis might lead to new treatments for these age-related symptoms. However, little is known about the molecular mechanism of elastic fiber assembly. We and others reported that mice deficient in a newly identified protein, developing arteries and neural crest EGF-like (DANCE) (also designated fibulin-5 or EVEC), exhibit a severely disorganized elastic fiber system throughout the body (Nakamura *et al*, 2002; Yanagisawa *et al*, 2002). DANCE is a secreted 66-kDa molecule, which colocalizes with elastic fibers and is abundantly expressed in developing arteries (Nakamura *et al*, 1999). We have recently demonstrated that DANCE has an elastogenic organizer activity, by showing that recombinant DANCE can induce elastogenesis in cell culture (Hirai *et al*, 2007). DANCE deposits on microfibrils, then promotes coacervation and crosslinking of tropoelastin molecules along microfibrils. Thus, DANCE is not only necessary for elastogenesis, but also able to promote elastic fiber organization. Therefore, DANCE may provide important clues to the molecular basis of elastogenesis.

Elastic fibers are known to consist of two morphologically distinct components: microfibrils and polymerized elastin (Rosenbloom *et al*, 1993). Microfibrils are 10–12 nm filaments in the extracellular matrices, and mainly consist of large extended glycoproteins, fibrillin-1 and -2 (Sakai *et al*, 1986; Zhang *et al*, 1994), together with several kinds of proteins that are associated with them, such as latent transforming growth factor β-binding proteins (LTBPs) (Gibson *et al*, 1995; Taipale *et al*, 1995) and microfibril-associated glycoproteins (MAGPs) (Gibson *et al*, 1986, 1996). Microfibrils are considered to provide a scaffold for the orientated deposition of tropoelastin monomers and to play a central role in elastogenesis, although they can also form macroaggregates devoid of elastin (Ramirez *et al*, 2004). The expression of fibrillin-1 and -2 is differentially controlled, but overlaps in the development of elastic tissues (Mariencheck *et al*, 1995). Although fibrillin-1-mutated mice develop normal elastic matrices (Pereira *et al*, 1997) and fibrillin-2-mutated mice show syndactyly but normal elastogenesis (Arteaga-Solis *et al*, 2001; Chaudhry *et al*, 2001), mice deficient in both fibrillin-1 and -2 were recently reported to exhibit impaired elastogenesis (Carta *et al*, 2006). However, why only a part of microfibrils deposit elastin to form elastic fibers and how fibrillin-1 and -2 microfibrils are differentially utilized in elastogenesis remains unclear. These considerations prompted us to investigate whether there might be any microfibril molecules that regulate elastic fiber assembly. For example, LTBP proteins share a high degree of homology with fibrillins. There are four isoforms in the LTBP family (LTBP-1, -2, -3, and -4) (Kanzaki *et al*, 1990; Moren *et al*, 1994; Yin *et al*, 1995; Giltay *et al*, 1997; Saharinen *et al*, 1998; Hyytiainen *et al*, 2004). This

*Corresponding author. Department of Pharmacology, Kansai Medical University, 10-15, Fumizono-cho, Moriguchi, Osaka, 570-8506, Japan. Tel.: +81 6 6993 9427; Fax: +81 6 6993 9428;
E-mail: nakamtom@takii.kmu.ac.jp
[5]These authors contributed equally to this work

Received: 23 January 2007; accepted: 21 May 2007; published online: 21 June 2007

family is named based on its ability to bind the latent form of transforming growth factor-β (TGF-β) and to modulate TGF-β bioactivity, but the family members also serve as structural components of extracellular matrices. Notably, LTBP-2 has the distinctive characteristic that it cannot interact with TGF-β, whereas LTBP-1, -3, and -4 can interact with TGF-β (Saharinen and Keski-Oja, 2000). In addition, LTBP-2 is reported to be specifically localized to the elastin-associated microfibrils (Gibson *et al*, 1995). These findings suggest that LTBP-2 may play an important role in elastogenesis unrelated to the regulatory function of TGF-β activity.

To elucidate the molecular mechanisms of elastic fiber assembly and the roles of DANCE in elastogenesis, we attempted here to identify DANCE-binding proteins. Several groups have previously identified some DANCE-binding proteins, such as elastin (Yanagisawa *et al*, 2002; Freeman *et al*, 2005), lysyl oxidase-like 1 (Liu *et al*, 2004), EMILIN (Zanetti *et al*, 2004), apolipoprotein(a) (Kapetanopoulos *et al*, 2002), and extracellular superoxide dismutase (Nguyen *et al*, 2004). However, it is still not possible to fully understand the role that DANCE plays in elastic fiber development. In the present study, we demonstrate the interaction of DANCE and LTBP-2. We show that the middle calcium-binding epidermal growth factor-like domain (cbEGF-like domain) of DANCE specifically interacts with the amino- (N-) terminal domain of LTBP-2. Knockdown experiments using small interfering RNA (siRNA) reveal that deposition of DANCE and elastin is dependent on fibrillin-1, not on either fibrillin-2 or LTBP-2. Intriguingly, downregulation of LTBP-2 rescues fibrillar deposition of DANCE and elastin onto fibrillin-2 or other potential microfibrils, even in the absence of fibrillin-1. Moreover, recombinant LTBP-2 protein promotes fibrillar deposition of DANCE onto fibrillin-1 microfibrils. These results imply that LTBP-2 may function not only as a structural protein, but also as a regulatory protein that determines which microfibrils DANCE should deposit on for subsequent assembly of elastic fiber components.

Results

Latent TGF-β-binding protein-2 as a DANCE-binding protein

To clarify the molecular role of DANCE in elastogenesis, we attempted to identify DANCE-binding proteins. For this purpose, we performed immunoprecipitation/SDS–PAGE. Bovine aortic smooth muscle cells were metabolically labeled with ^{35}S-cysteine/methionine overnight, and the conditioned medium was harvested. An aliquot of the conditioned medium was combined with a purified FLAG-tagged DANCE recombinant protein or a mock control, followed by immunoprecipitation with a monoclonal anti-FLAG antibody. Other aliquots were subjected to immunoprecipitation with available antibodies against elastic fiber components, including elastin, fibrillin-1, fibrillin-2, and latent TGF-β-binding protein-2 (LTBP-2), to see whether there are these proteins in the conditioned medium. The immunoprecipitated complexes were separated by SDS–PAGE, and three major bands were detected as candidates for DANCE-binding proteins compared with the mock control (Figure 1, compare lanes 1 and 2, asterisks). The molecular weights of two of these bands are higher than 182 kDa, and that of the other is approximately 60 kDa (lane 2). We assumed that the larger molecules might

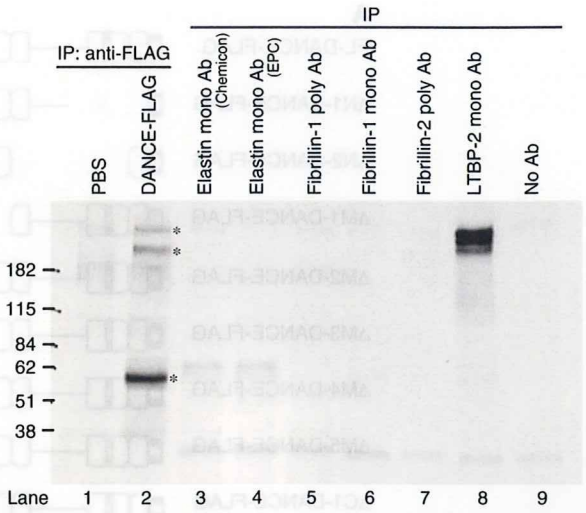

Figure 1 Latent TGF-β-binding protein-2 (LTBP-2) as a candidate DANCE-binding protein. Bovine smooth muscle cells were metabolically labeled with ^{35}S-cysteine/methionine, and conditioned media were subjected to immunoprecipitation. Several DANCE-binding proteins are detected (lane 2, asterisks). The sizes of the bands larger than 182 kDa are similar to those of proteins precipitated with anti-LTBP-2 antibody (compare lanes 2 and 8). Another 60-kDa band is inferred to be DANCE, which is abundantly expressed in aortic smooth muscle cells (lane 2).

be LTBP-2, because the molecular weight seems to be very similar to that of the protein immunoprecipitated with a monoclonal anti-LTBP-2 antibody (Figure 1, compare lanes 2 and 8). Fibrillin-1 and -2 were not detected, suggesting that these antibodies might not react with bovine fibrillin-1 and -2. In an analogous experiment using neonatal skin fibroblasts from wild-type mice, we found similar bands precipitated with the recombinant DANCE (data not shown). However, the 60-kDa band was not detected in the DANCE$^{-/-}$ neonatal fibroblast culture medium (data not shown); therefore, we infer that the 60-kDa molecule may be the DANCE itself, which is abundantly expressed in aorta (lane 2). To see whether these larger molecules are LTBP-2, we carried out double immunostaining of human skin fibroblasts with monoclonal antibodies against DANCE and LTBP-2. The result reveals that these two molecules colocalize, which suggests that they interact each other (Supplementary Figure S1).

LTBP-2 specifically interacts with the sixth calcium-binding EGF-like domain of DANCE

To examine whether DANCE actually interacts with LTBP-2, we performed *in vitro* binding assays. Myc-tagged LTBP-2 proteins overexpressed by 293T cells were incubated with FLAG-tagged DANCE or a series of FLAG-tagged DANCE deletion mutant proteins (Figure 2A) also overexpressed by 293T cells. Each mixture was subjected to immunoprecipitation with anti-FLAG antibody, and then Myc-tagged proteins associated with the FLAG-tagged proteins were detected by Western blotting. As shown in Figure 2B, DANCE interacts with LTBP-2 (compare lane 1 with 11). Among the deletion mutant proteins, ΔM5-DANCE does not interact with LTBP-2 at all (Figure 2B, upper panel, lane 8). This result indicates that DANCE directly interacts with LTBP-2 through the sixth cbEGF-like domain. The carboxy- (C-) terminal domain of

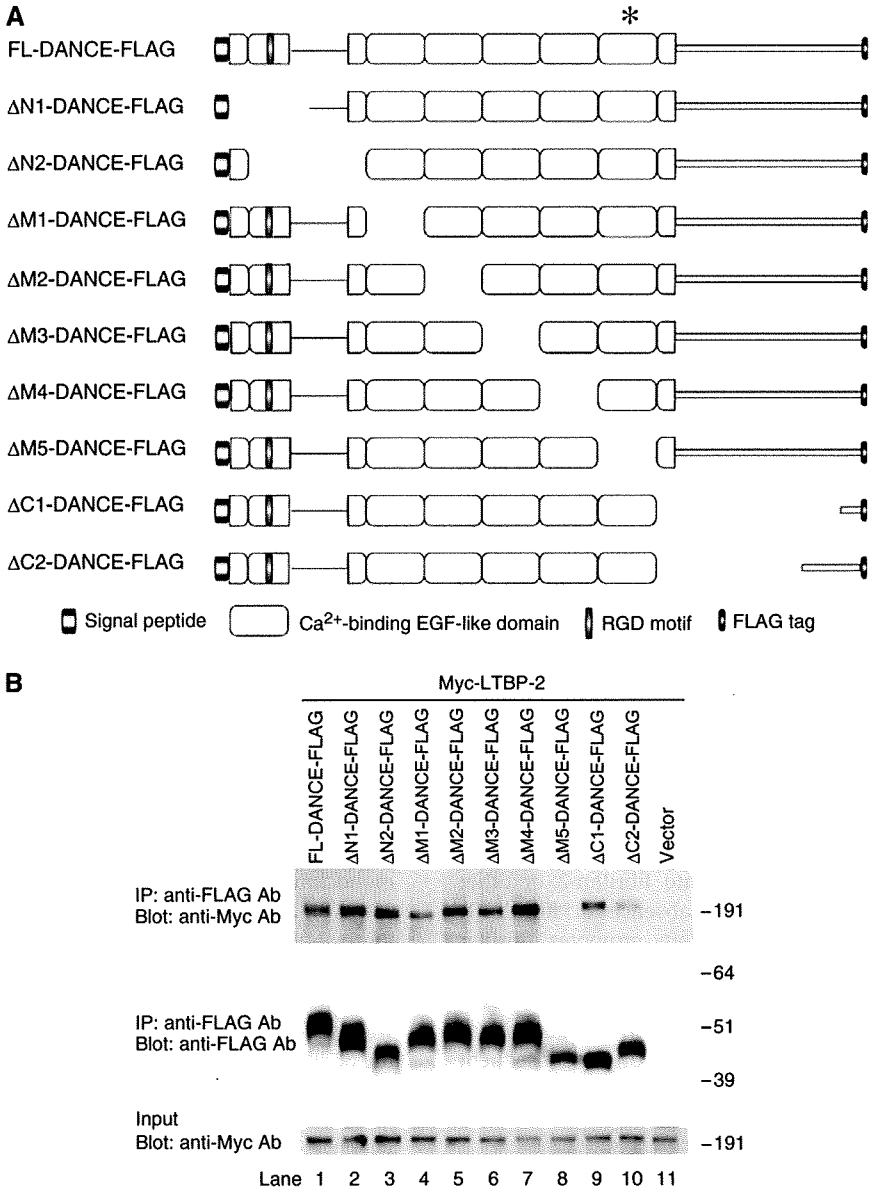

Figure 2 Schematic representation of the DANCE deletion mutants, and mapping of the binding domain of DANCE with LTBP-2. (**A**) Domain structure of the full-length DANCE and the DANCE deletion mutants used for the *in vitro* binding assay. These mutants were expressed as C-terminally FLAG-tagged proteins. We prepared expression vectors encoding FLAG-tagged DANCE (FL-DANCE-FLAG) or DANCE deletion mutants, including N-terminal domain deletion mutants (ΔN1- and ΔN2-DANCE-FLAG), central calcium-binding EGF (cbEGF)-like repeat domain deletion mutants (ΔM1-, ΔM2-, ΔM3-, ΔM4-, and ΔM5-DANCE-FLAG), and C-terminal domain deletion mutants (ΔC1- and ΔC2-DANCE-FLAG). The asterisk indicates the sixth cbEGF-like domain of DANCE, where LTBP-2 binds. (**B**) The sixth cbEGF-like domain of DANCE interacts with LTBP-2. 293T cells were transiently transfected with the vectors shown in A or mock vector. Expression vectors for Myc-tagged full-length LTBP-2 (LTBP-2-Myc) were also independently transfected into 293T cells. Transfected cells were cultured in serum-free medium for 48 h, and then the cell lysates and the conditioned media were harvested and mixed. After incubation of LTBP-2-Myc with a set of FLAG-tagged DANCE deletion mutants, each mixture was subjected to immunoprecipitation with anti-FLAG antibody. These immunoprecipitates were then separated by SDS–PAGE, and analyzed by Western blotting with a monoclonal anti-Myc antibody.

DANCE may also be involved in the interaction, as the binding of ΔC1- and ΔC2-DANCE with LTBP-2 was weaker than that of full-length DANCE with LTBP-2.

To see whether DANCE deletion mutants maintain their structural integrity, we performed a solid phase binding assay on recombinant tropoelastin. The result shows that ΔM5-DANCE binds tropoelastin as strongly as full-length DANCE (Supplementary Figure S2). We also carried out a deglycosylation assay using N-glycosidase F. Incubating ΔM5-DANCE with glycosidase did not change its molecular size, whereas the same glycosidase treatment caused size reduction of ΔM4-DANCE to a similar size of ΔM5-DANCE (Supplementary Figure S3). Taking into account that the sixth cbEGF-like domain contains putative N-glycosilation site (Nakamura *et al*, 1999) and that both mutants miss one cbEGF-like domain, this result indicates that not only ΔM4-DANCE, but also other DANCE mutants are properly processed after translation as well as the full-length DANCE.

DANCE interacts with the N-terminal domain of LTBP-2

To identify the DANCE-binding domain in the LTBP-2 molecule, we constructed expression vectors encoding five types of LTBP-2 truncation mutants with FLAG-tag (LTBP-2-A-FLAG through LTBP-2-E-FLAG, Figure 3A). FLAG-tagged LTBP-2 truncation mutants and Myc-tagged full-length DANCE recombinant proteins were transiently expressed in 293T cells, and were subjected to *in vitro* binding assays. As shown in Figure 3B (left panel), only LTBP-2-A fragment can interact with DANCE (lane 2). This result demonstrates that DANCE specifically interacts with the N-terminal domain of LTBP-2.

To more precisely identify the domain of LTBP-2 involved in this interaction, we constructed two expression vectors encoding FLAG-tagged LTBP-2-F and -G fragments by dividing the LTBP-2-A fragment (Figure 3A). As shown in Figure 3B (right panel), *in vitro* binding assays reveal that DANCE specifically interacts with LTBP-2-G fragment (lane 10), but not with LTBP-2-F fragment (lane 9). We further constructed expression vectors encoding FLAG-tagged LTBP-2-H and -I fragments by dividing the LTBP-2-G fragment (Figure 3A). Because the LTBP-2-H fragment is easily degraded, we constructed immunoglobulin fusion proteins to prevent degradation (LTBP-2-G-Ig, LTBP-2-H-Ig, and LTBP-2-I-Ig). DANCE interacted with the immunoglobulin-fused LTBP-2-G-Ig, as well as the intact LTBP-2-G fragment, indicating that the fused immunoglobulin does not affect the interaction with DANCE (Figure 3B, compare lanes 10 and 11). As shown in Figure 3B, *in vitro* binding assays revealed that DANCE specifically interacts with the LTBP-2-I-Ig, but not with the LTBP-2-H-Ig (Figure 3B, lanes 12 and 13). These results demonstrate that DANCE specifically interacts with the second four-cysteine repeat of LTBP-2.

Next, we examined the Ca^{2+} dependency of the interaction between DANCE and LTBP-2. Myc-tagged LTBP-2 and FLAG-tagged DANCE recombinant proteins were expressed in 293T cells, and subjected to *in vitro* binding assays in the presence or absence of EDTA (ethylenediaminetetraacetic acid). As shown in Figure 3C, the interaction between DANCE and LTBP-2 was markedly diminished in the presence of 1 mM EDTA, and almost abolished in the presence of 2 mM EDTA (Figure 3C, upper panel, lanes 1–3). These results indicate that the DANCE–LTBP-2 interaction is likely to be Ca^{2+} dependent, which is consistent with our finding that LTBP-2 interacts with the Ca^{2+}-binding EGF (cbEGF)-like domain of DANCE, whereas the N-terminal domain of LTBP-2 does not contain any cbEGF domain.

DANCE interacts with LTBP-2 in vivo

To investigate whether DANCE colocalizes with LTBP-2 at the tissue level, we performed *in situ* hybridization using neonatal mice. As shown in Figure 4A and B, both the DANCE transcript and the LTBP-2 transcript are strongly detected in the cardiac outflow tract, cardiac valves, aorta, and lung. The expression patterns of these two transcripts are strikingly similar, except for the minor difference that DANCE is more strongly expressed in arteries than in lung distal airspace walls, whereas the expression of LTBP-2 is similar in these tissues. These expression patterns suggest that DANCE is localized in close proximity to LTBP-2 *in vivo*.

To examine the interaction of DANCE and LTBP-2 *in vivo*, we performed co-immunoprecipitation analysis using lung extracts from wild-type and DANCE$^{-/-}$ mice. Immunoreactive DANCE protein was precipitated from lung extracts with anti-DANCE antibody followed by Western blotting using an anti-LTBP-2 antibody. As shown in Figure 5, the interaction of DANCE and LTBP-2 was detected (upper panel, compare lanes 1, 2 and lanes 3, 4). This result indicates that endogenous DANCE interacts with endogenous LTBP-2 *in vivo*.

BIAcore analysis of the interaction between DANCE and LTBP-2

To investigate the affinity of the binding of DANCE to LTBP-2, we performed kinetic analyses using surface plasmon resonance with a Biacore X instrument. The proteins used for the assay were purified from 293T cell lines stably overexpressing C-terminal histidine-tagged full-length DANCE and LTBP-2. Analysis by SDS–PAGE followed by Coomassie blue staining revealed that the purities of these proteins were more than 80% (Figure 6A). The purified DANCE recombinant protein was immobilized on a CM5 sensor chip, and LTBP-2 was used as the analyte. Kinetic analyses were performed at a range of concentrations of 15–360 μg/ml (75–1800 nM) of LTBP-2 on the DANCE-immobilized chip, and the dissociation constant (K_D) of the binding of LTBP-2 to DANCE was determined to be 265 nM, which indicates that this interaction is direct and specific (Figure 6B).

Deposition of DANCE is dependent on fibrillin-1, not on either fibrillin-2 or LTBP-2

To investigate the physiological significance of the interaction of DANCE and LTBP-2, we used RNA interference (RNAi) to knock down target genes. For this purpose, we developed an *in vitro* culture system of human skin fibroblasts to assess the

Figure 3 Schematic representation of the LTBP-2 truncation mutants, and mapping of the binding domain of LTBP-2 with DANCE. (**A**) Domain structure of the full-length LTBP-2 and the LTBP-2 truncation mutants used for the *in vitro* binding assay. These mutants were expressed as N-terminally FLAG-tagged proteins flanked by the preprotrypsin signal sequence, except for the full-length LTBP-2. The LTBP-2-H fragment is prone to degradation, so we constructed C-terminal fusion proteins with the constant region of human IgG to prevent the degradation (LTBP-2-G-Ig, LTBP-2-H-Ig, and LTBP-2-I-Ig). The characteristics of each domain are described below the figure. The asterisk indicates the second four-cystein domain of LTBP-2, where DANCE binds. (**B**) Left panel, DANCE interacts with the N-terminal domain of LTBP-2 (LTBP-2-A). Right panel, DANCE interacts with the second four-cysteine domain of LTBP-2 (LTBP-2-I). The expression vector of each LTBP-2 truncation mutant was transfected into 293T cells. Mixtures of the media and cell lysates of FLAG-tagged LTBP-2 truncation mutants were incubated with DANCE-Myc, and then these reactants were subjected to immunoprecipitation with anti-FLAG antibody. The immunoprecipitates were separated by SDS–PAGE, and analyzed by Western blotting with anti-Myc antibody. (**C**) Calcium dependency of the LTBP-2–DANCE interaction. The expression vector for Myc-tagged full-length LTBP-2 was transfected into 293T cells. Mixtures of the conditioned media and cell lysates of Myc-LTBP-2 were incubated with the conditioned media of DANCE-FLAG in the presence of EDTA (0, 1, 2, 5, or 10 mM). These cocktails were subjected to immunoprecipitation with anti-FLAG antibody. The immunoprecipitates were separated by SDS–PAGE, and analyzed by Western blotting with anti-Myc antibody.

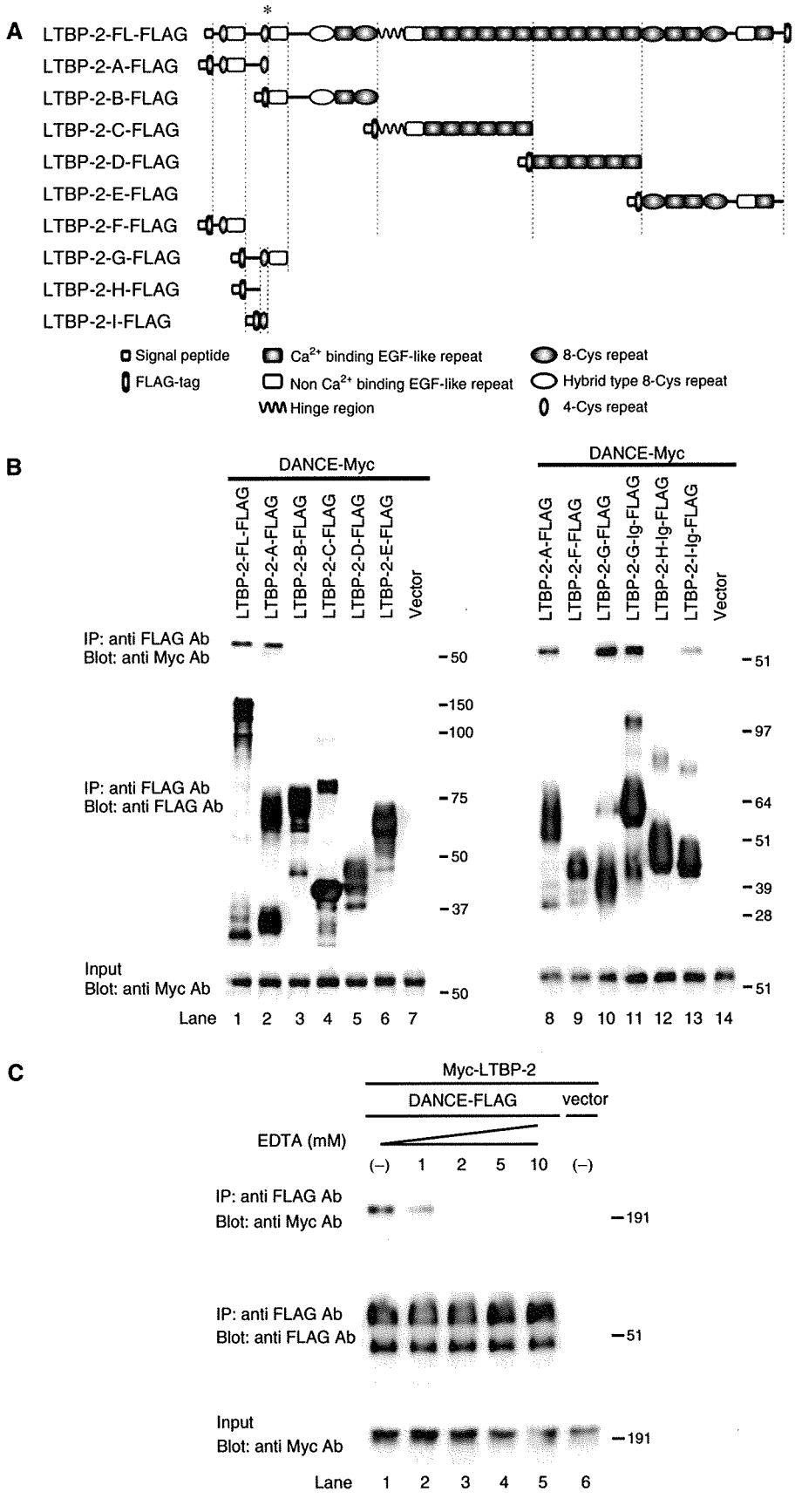

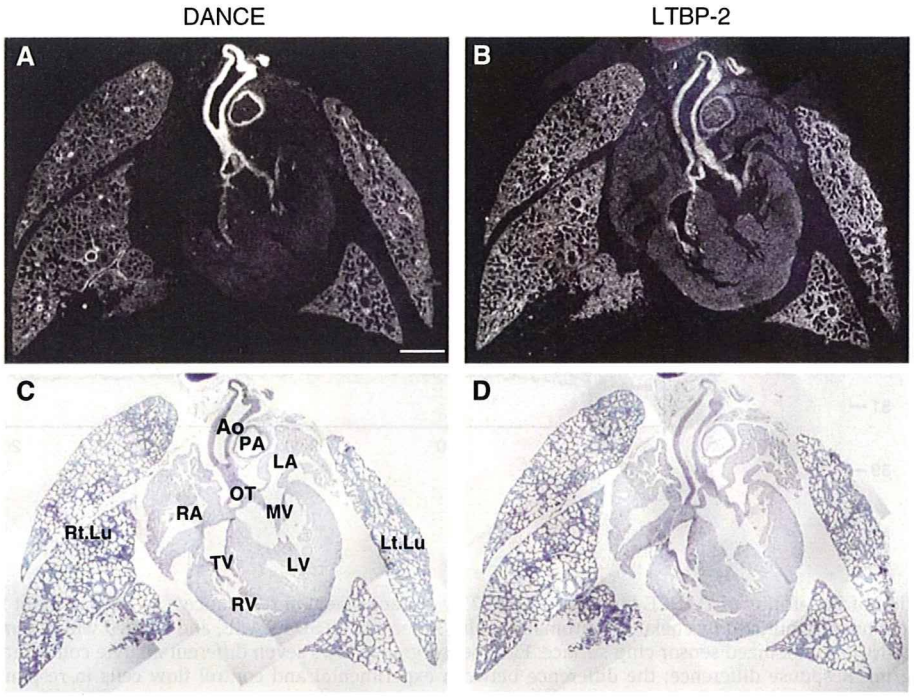

Figure 4 Expression patterns of DANCE (**A**) and LTBP-2 (**B**) transcripts in neonatal mice as shown by *in situ* hybridization with dark field (A, B) and bright field (**C, D**) views. Ao, aorta; PA, pulmonary artery; OT, cardiac outflow tract; MV, mitral valve; TV, tricupsid valve, LV, left ventricle; RV, right ventricle; LA, left atrium; RA, right atrium; Rt.Lu, right lung; Lt.Lu, left lung. Scale bar; 500 μm.

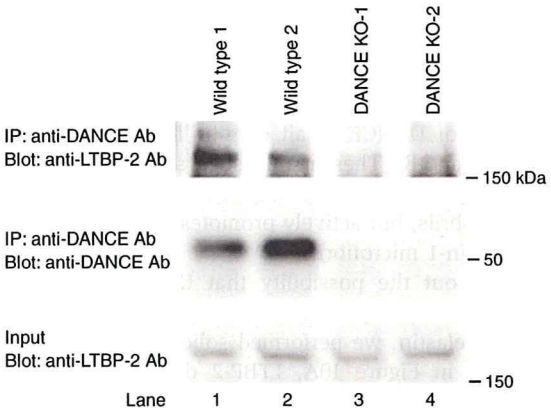

Figure 5 DANCE interacts with LTBP-2 *in vivo*. Whole lungs were dissected from two lines each of wild-type and DANCE-deficient mice. Proteins were extracted using a homogenizer on ice. Immunoreactive DANCE protein was precipitated from lung extracts with anti-DANCE antibody, followed by Western blotting with a polyclonal anti-LTBP-2 antibody.

effects of gene knockdown on elastic fiber assembly. We reverse transfected each siRNA duplex into human skin fibroblasts, cultured the transfected cells in 10% serum-containing medium for more than 10 days, and subjected them to immunostaining with anti-elastin and anti-DANCE antibody. As controls, we used siRNA with a scrambled sequence of protein phosphatase PP2C gamma, a gene irrelevant to the extracellular matrix. Because LTBP-2 is a constituent of elastic microfibrils, we also examined the role of fibrillin-1 and -2, major constituents of elastic microfibrils, in addition to LTBP-2. We confirmed that treatment with siRNA results in more than a 90% decrease in the respective transcripts even in double or triple knockdown cells as detected by quantitative polymerase chain reaction (qPCR) (Figure 7A). No off-target knockdown was observed at least in mRNAs of fibrillin-1 and -2, LTBP-2, DANCE and elastin (data not shown). Fibrillin-1 and -2 knockdown specifically abolished each meshwork of fibrillin-1 and -2 microfibrils (Figure 7B–O). As shown in Figure 8B, fibrillin-1-knockdown cells develops only a faint meshwork of elastic fibers, whereas fibrillin-2-knockdown cells and LTBP-2-knockdown cells each develop abundant meshworks of elastic fibers like those in the control cells (Figure 8A, C and D). Moreover, DANCE is barely deposited on fibrillin-1-knockdown cells (Figure 8J), whereas DANCE is abundantly deposited and colocalizes with elastin on fibrillin-2- or LTBP-2-knockdown cells (Figure 8I, K and L). These results indicate that DANCE and elastin are deposited mainly on fibrillin-1 microfibrils in human skin fibroblast culture.

LTBP-2 inhibits fibrillin-1-independent deposition of DANCE and elastin

Next, we investigated the role of LTBP-2 in the deposition of DANCE in the absence of fibrillin-1. For this purpose, we doubly knocked down LTBP-2 in addition to fibrillin-1. As shown in Figure 8E and M, the nearly abolished deposition of DANCE and elastin resulting from fibrillin-1 knockdown is unexpectedly rescued by additional LTBP-2 knockdown. The rescue effect of LTBP-2 knockdown is similar when each of three different siRNAs to LTBP-2 is independently transfected with fibrillin-1 siRNA (data not shown). To rule out off-target effects of LTBP-2 RNAi, we added recombinant LTBP-2 protein to these fibrillin-1–LTBP-2 double knockdown cells. As shown in Figure 8F and N, addition of recombinant LTBP-2

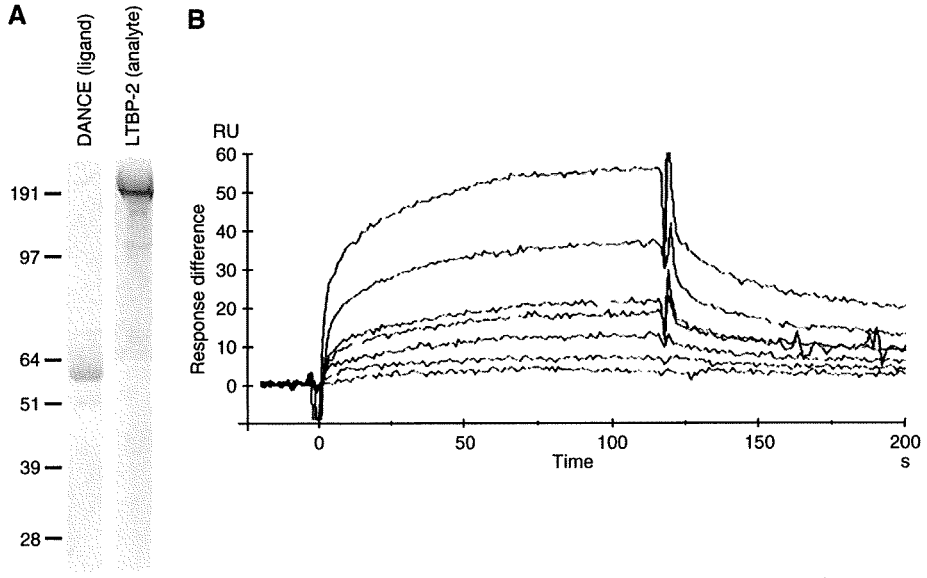

Figure 6 Quantification of the affinity of DANCE binding to LTBP-2 by surface plasmon resonance. (**A**) Recombinant full-length DANCE and full-length LTBP-2 proteins were purified by chelating chromatography, separated by SDS–PAGE, and stained with Coomassie Blue. (**B**) LTBP-2 was injected over a DANCE-immobilized sensor chip surface. Each sensorgram shows seven different analyte concentrations of 15, 30, 60, 90, 180, 240, and 360 μg/ml. Response difference; the difference between experimental and control flow cells in response units (RU). Time is shown in seconds (s).

greatly reduces the deposition of DANCE and elastin to a similar level as observed in fibrillin-1 single knockdown cells. These results indicate that the rescue phenotype in double-knockdown cells is specifically due to depletion of LTBP-2, which implies that LTBP-2 inhibits fibrillin-1-independent deposition of DANCE and elastin.

Next, we asked whether DANCE is deposited on fibrillin-2 microfibrils instead of fibrillin-1 microfibrils, in the fibrillin-1–LTBP-2 double knockdown culture. To investigate this possibility, we examined the effect of fibrillin-1–fibrillin-2–LTBP-2 triple knockdown. The deposition of DANCE and elastin on fibrillin-1–fibrillin-2–LTBP-2 triple-knockdown cells is substantially less than that on fibrillin-1–LTBP-2 double-knockdown cells (Figure 8E, H, M and P). These results suggest that downregulation of LTBP-2 causes deposition of DANCE and elastin mainly on fibrillin-2 microfibrils. Moreover, it is possible that there might be potential microfibrils devoid of fibrillin-1 and -2 on which DANCE and elastin can be deposited in the absence of LTBP-2, because we detected weak, but more considerable fibrillar deposition of DANCE and elastin on fibrillin-1–fibrillin-2–LTBP-2 triple-knockdown cells than on fibrillin-1–fibrillin-2 double-knockdown cells (Figure 8G, H, O and P). We could not, however, rule out a possibility that even an undetectable amount of fibrillin-1 or -2 might support deposition of DANCE and elastin in the absense of LTBP-2. These data suggest that LTBP-2 inhibits fibrillin-1-independent deposition of DANCE and elastin onto fibrillin-2 or other potential microfibrils.

Recombinant LTBP-2 protein promotes deposition of DANCE onto fibrillin-1 microfibrils

Because LTBP-2 inhibits fibrillin-1-independent deposition of DANCE, we hypothesized that LTBP-2 may promote deposition of DANCE on fibrillin-1 microfibrils. To test this hypothesis, we added recombinant LTBP-2 into the medium of fibrillin-1, -2, or control-knockdown cells, cultured them in 5% serum-containing medium and subjected them to immunostaining with anti-DANCE and anti-fibrillin-1 antibody. As shown in Figure 9, recombinant LTBP-2 markedly increases the deposition of DANCE in fibrillin-2-knockdown cells (Figure 9C and D). On the other hand, we cannot detect deposition of DANCE at all on fibrillin-1-knockdown cells (Figure 9A and B). These results suggest that LTBP-2 not only inhibits deposition of DANCE onto fibrillin-2 or other potential microfibrils, but actively promotes deposition of DANCE onto fibrillin-1 microfibrils.

To rule out the possibility that LTBP-2 might regulate deposition of tropoelastin through direct interaction with tropoelastin, we performed solid phase binding assay. As shown in Figure 10A, LTBP-2 does not interact with tropoelastin at all, whereas DANCE strongly interacts with tropoelastin.

These data suggest a model on the role of DANCE–LTBP-2 interaction in elastic fiber assembly (Figure 10B and C): binding of LTBP-2 to DANCE promotes DANCE deposition on fibrillin-1 and inhibits DANCE deposition on fibrillin-2 or other potential microfibrils.

Discussion

The DANCE molecule has been shown to play an integral role in elastic fiber development. Identification of the roles of DANCE-binding proteins may lead to new understanding of the molecular mechanisms of elastic fiber assembly. In the present study, we newly demonstrate the interaction of DANCE and LTBP-2. LTBP-2 is known to associate with elastic tissue microfibrils and has been considered to perform a structural role within elastic fibers (Gibson *et al*, 1995). The distributions of DANCE and LTBP-2 transcripts are shown by *in situ* hybridization to strikingly coincide. The interaction of

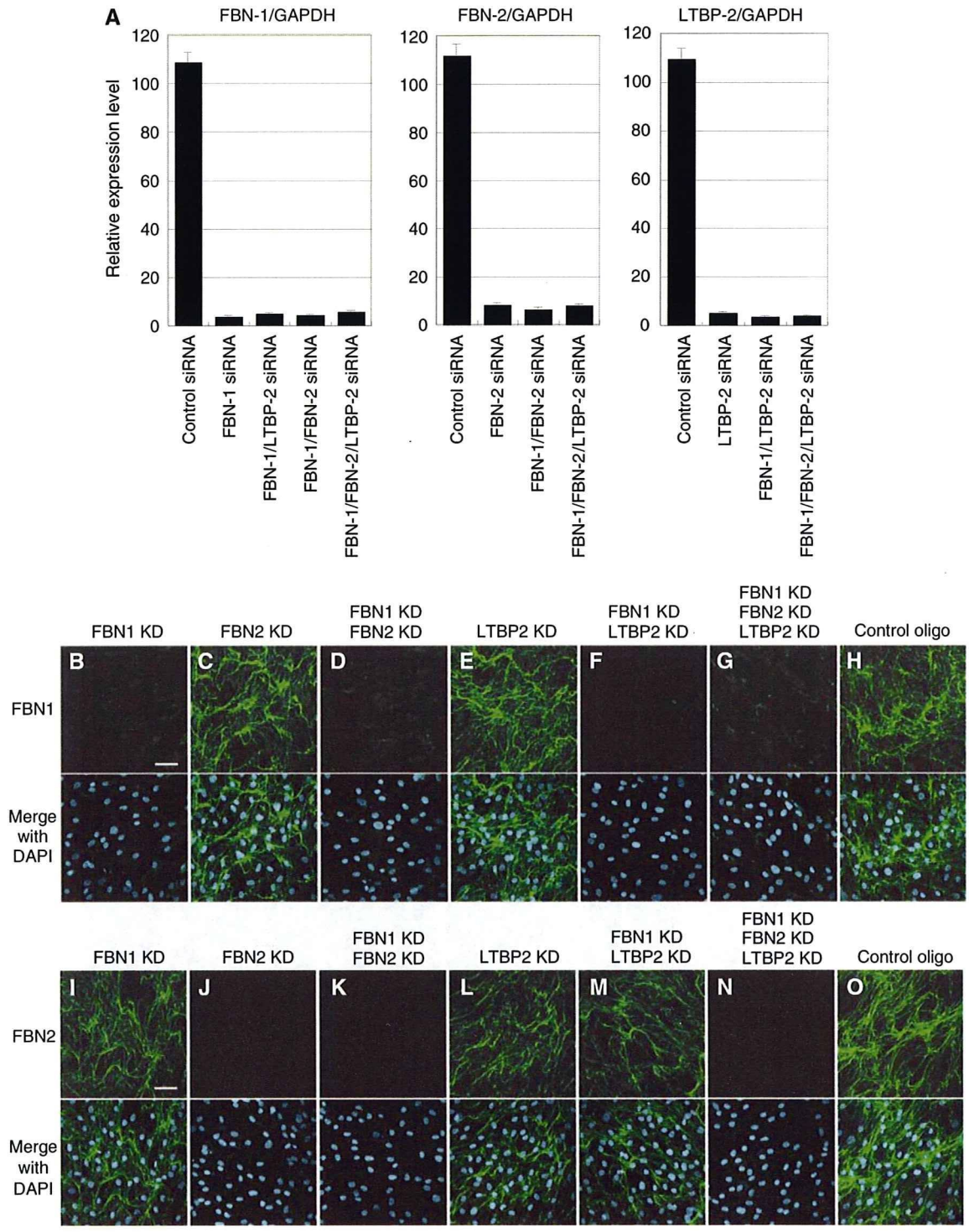

Figure 7 Quantitative PCR analysis of gene knockdown in skin fibroblasts (**A**), and fibrillin-1 and -2 knockdown specifically abolishes the meshwork of fibrillin-1 and -2 microfibrils, respectively (**B–O**). (A) Total RNA from siRNA-transfected skin fibroblasts was extracted 9 days after transfection. Complementary DNA was synthesized and was subjected to quantitative real-time PCR for the expression of fibrillin-1, fibrillin-2, LTBP-2, and glyceraldehyde-3-phosphate dehydrogenase (GAPDH) transcripts. A graphic presentation of the results obtained by qPCR is shown. Levels of GAPDH transcript are used to normalize the cDNA levels. The relative amount of the PCR product amplified from control siRNA-treated fibroblasts is set at 100. Data are presented as the means ± s.e. of three independent experiments, each performed in duplicate. (B–O) HSFs were transfected with each RNAi oligo as indicated and cultured in 10% serum containing media. Cells were stained with anti-fibrillin-1 (B–H) or anti-fibrillin-2 antibody (I–O). Lower panels are superimpositions of upper panels with DAPI (4,6-diamidino-2-phenylindole) nuclear staining. KD, knockdown; FBN-1, fibrillin-1; FBN-2, fibrillin-2. Scale bars; 60 μm.

endogenous DANCE and LTBP-2 is demonstrated in mice organs by co-immunoprecipitation. Kinetic analysis reveals that the affinity of this interaction is potent and specific. We mapped the specific binding domain of these molecules and show that the sixth cbEGF-like domain of DANCE interacts with the N-terminal domain of LTBP-2. This N-terminal LTBP-2 domain has been suggested to be important for the interaction of LTBP-2 and extracellular matrices (Hyytiäinen *et al*,

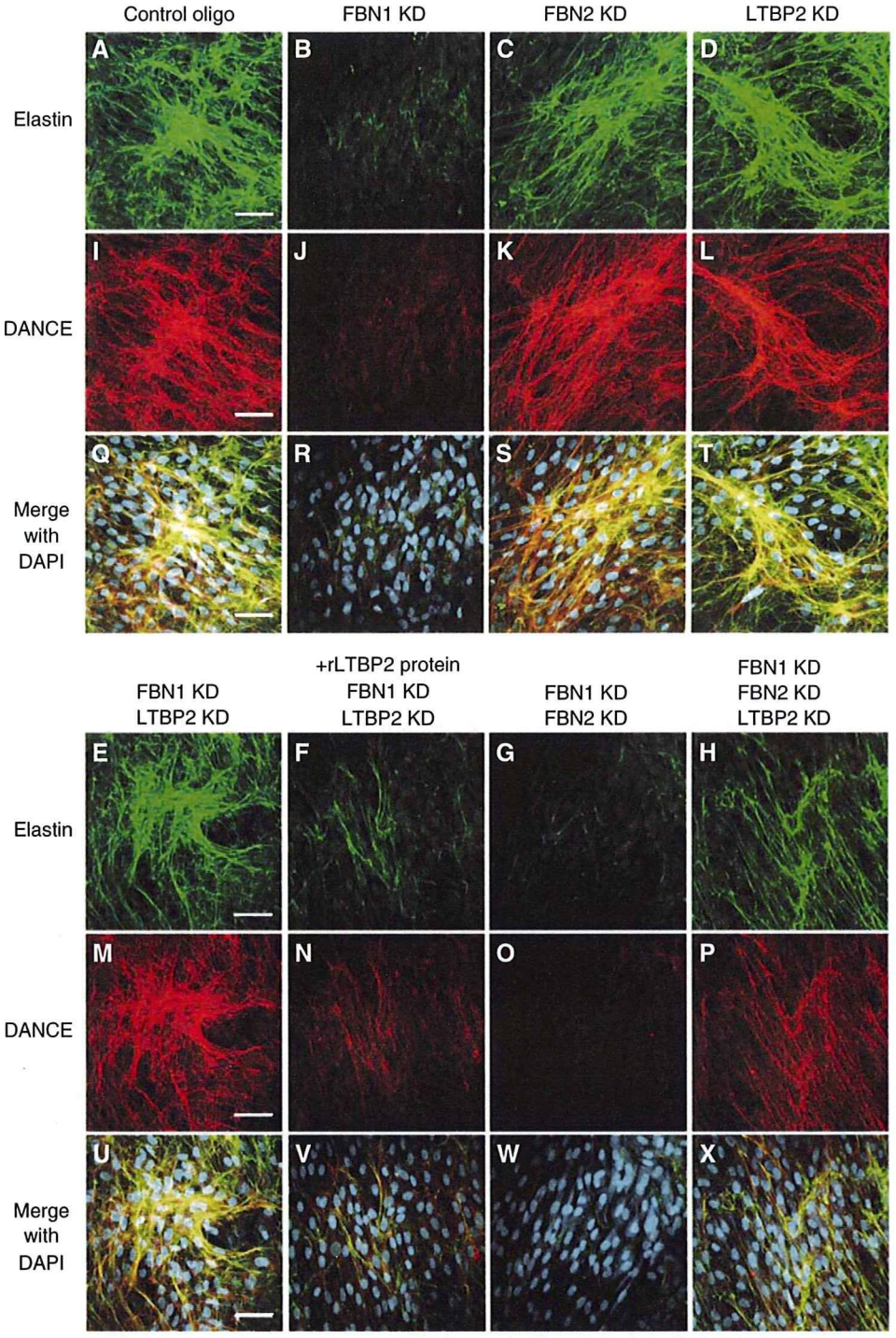

Figure 8 DANCE and elastin deposition is dependent on fibrillin-1 microfibril, but LTBP-2 knockdown induces fibrillin-1-independent deposition of DANCE and elastin. HSFs were transfected with each RNAi oligo as indicated, cultured in 10% serum containing media for 14 days and fixed. Cells were stained with anti-elastin (**A–H**) and anti-DANCE (**I–P**) antibodies. In (F) and (N), recombinant LTBP-2 (rLTBP2) was added to the culture medium to cancel the knockdown effect of LTBP-2. (**Q–X**) Superimpositions of (A–H) and (I–P) with DAPI nuclear staining, showing that DANCE colocalizes with elastic fibers. Scale bars; 60 μm.

1998). To investigate the functional roles of LTBP-2, we set up an *in vitro* culture system with which we can evaluate the effects of gene knockdown in elastic fiber development. Using this system, we demonstrate that deposition of DANCE and elastin is dependent on fibrillin-1 in human skin fibroblast cell culture. We also demonstrate that downregulation of LTBP-2 can direct fibrillin-1-independent deposition of DANCE and elastin, whereas recombinant LTBP-2 can promote deposition of DANCE on fibrillin-1 microfibrils. These results suggest that LTBP-2 might work as a molecular switch that regulates the differential usage of microfibrils in elastic fiber assembly.

Fibrillin-1 is the major structural component of elastic microfibrils. We have found that deposition of DANCE is

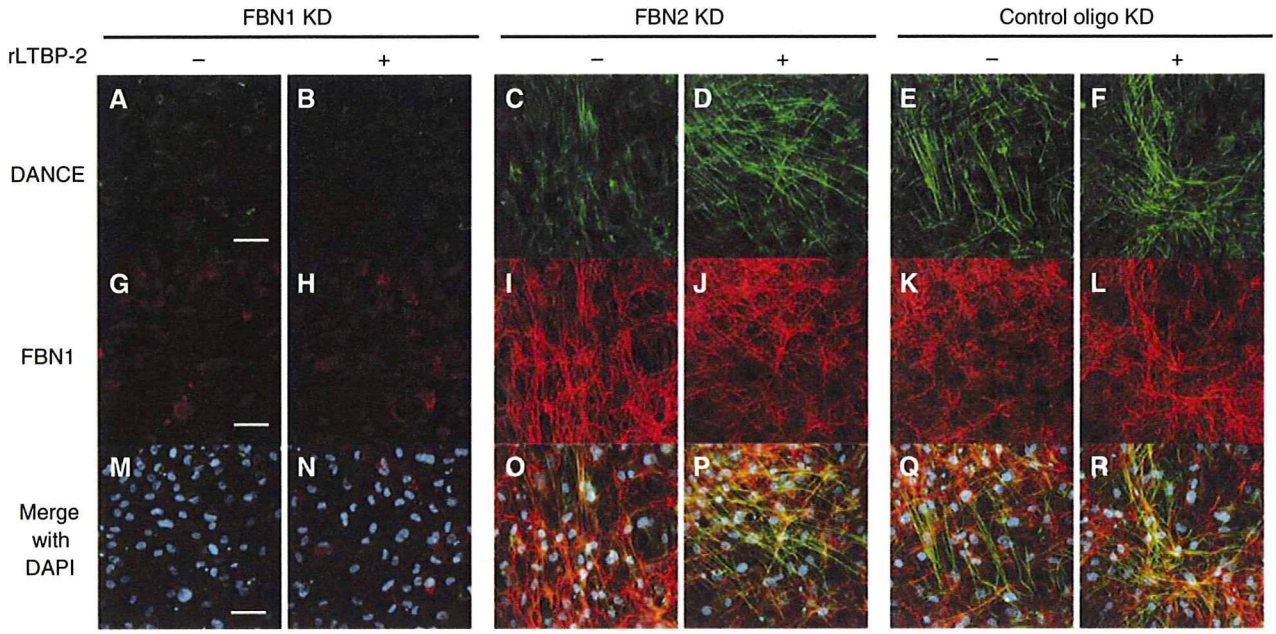

Figure 9 Recombinant LTBP-2 markedly increases deposition of DANCE onto fibrillin-1 microfibrils in fibrillin-2-knockdown cells. HSFs were transfected with each RNAi oligo as indicated, cultured in 5% serum containing media for 14 days and fixed. Two days after transfection, recombinant LTBP-2 protein (16 μg/ml) or mock was added to the culture medium. Cells were stained with anti-DANCE (**A–F**) and anti-fibrillin-1 (**G–L**) antibodies. (**M–R**) Superimpositions of (A–F) and (G–L) with DAPI nuclear staining. Scale bars; 60 μm.

dependent on fibrillin-1 in cell culture, which is consistent with a recent report showing that DANCE directly interacts with fibrillin-1 (Freeman *et al*, 2005). However, fibrillin-1-deficient mice are reported to develop normal elastic matrices, whereas DANCE-deficient mice show disorganized and fragmented elastic matrices (Pereira *et al*, 1997; Nakamura *et al*, 2002; Yanagisawa *et al*, 2002; Ramirez *et al*, 2004). Recent findings that fibrillin-1–fibrillin-2 double-deficient mice fail to complete fetal development with impaired elastogenesis suggest that fibrillin-2 can compensate for fibrillin-1 deficiency in elastic fiber development (Carta *et al*, 2006). In human skin fibroblast culture, however, we show that knockdown of fibrillin-1 is not compensated, even though there is abundant fibrillin-2 meshwork. It is often observed that more compensatory mechanisms work in the development than in cell culture. Further investigation is required to identify the compensatory mechanism between the fibrillins in embryogenesis, and to determine whether LTBP-2 is a part of the compensatory mechanism.

Although fibrillin-1 and -2 molecules are structurally similar glycoproteins, they are differentially expressed in terms of both developmental stages and tissue distribution. Fibrillin-2 is generally expressed in earlier gestational period than fibrillin-1, and the expression of fibrillin-2 coincides with the beginning of elastogenesis, leading to the idea that fibrillin-2 might play a role at early stage of elastogenesis, whereas fibrillin-1 might play a role at later stage (Zhang *et al*, 1995). Thus, fibrillins are differentially employed in the development of elastic matrices during embryogenesis. Here, we show that LTBP-2 may play an important role in regulating the differential usage of microfibrils from fibrillin-2 to fibrillin-1. Consistent with these findings, LTBP-2 transcripts start to express in elastic organs at a similar timing, when fibrillin-1 transcripts gradually increases on around 13.5 days postcoitum (Nunes *et al*, 1997; Shipley *et al*, 2000). On the other hand, microfibrils have been reported to be often composites of fibrillin-1 and -2 in skin fibroblasts culture (Charbonneau *et al*, 2003). LTBP-2 does not seem to either inhibit or promote deposition of DANCE onto these microfibrils (Figure 9E and F).

LTBP-2 has been shown to be specifically localized in elastin-containing microfibrils (Gibson *et al*, 1995). Moreover, the expression of LTBP-2 transcripts largely parallels that of tropoelastin transcripts (Shipley *et al*, 2000). On the other hand, fibrillin-1 is also observed in tissues devoid of elastin, and seems to play more redundant roles than elastic fiber matrices. In fact, immunostaining of elastin colocalizes with that of only a part of the fibrillin-1 microfibrils meshwork (Supplementary Figure S4). In contrast, the distributions of DANCE and elastin are quite similar (Figure 8A, I and Q). Therefore, among the meshwork of fibrillin-1 microfibrils, only microfibrils with DANCE deposition seem to develop mature elastic fibers. One intriguing possibility is that LTBP-2 can also be involved in the selection of fibrillin-1 microfibrils on which DANCE should be deposited. However, we cannot rule out the involvement of other molecules than LTBP-2, such as proteoglycans or other LTBP family members, in the process of DANCE deposition. LTBPs-1 and -2 have recently been shown to bind fibrillin-1 through their C-terminal region but not to fibrillin-2, which may account for the mechanism of LTBP-2 in the selection of fibrillins (Hirani *et al*, 2007). To clarify the precise role of LTBP-2 in elastic fiber assembly *in vivo*, further studies using conditional knockout mice will be needed, because LTBP-2-deficient mice are embryonic lethal at the implantation stage, due to a cause unrelated to elastic fibers (Shipley *et al*, 2000).

In summary, we have identified LTBP-2 as a DANCE-binding protein that can regulate DANCE deposition on microfibrils. We demonstrate that the DANCE and elastin deposition on microfibrils is dependent on fibrillin-1 in the

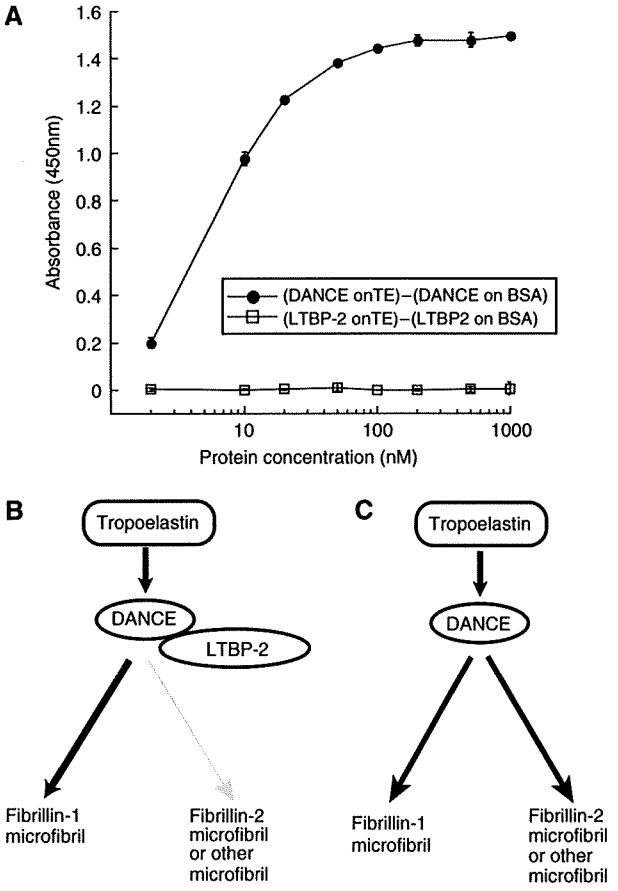

Figure 10 DANCE strongly interacts with tropoelastin, whereas LTBP-2 does not directly interact with tropoelastin (**A**), and working hypothesis on the role of LTBP-2 in elastic fiber assembly (**B, C**). (A) Solid phase binding assay on recombinant tropoelastin or bovine serum albumin (BSA) was performed using recombinant FLAG-tagged LTBP-2 or DANCE as a soluble ligand. LTBP-2 does not interact with tropoelastin at all, whereas DANCE definitely interacts with tropoelastin. Signals detected for binding on BSA are subtracted as nonspecific background. All measurements were performed in triplicate, and values shown are means±s.d. (B, C) Schematic illustration of our hypothesis. LTBP-2 promotes deposition of DANCE onto fibrillin-1 microfibrils, whereas inhibiting deposition of DANCE on fibrillin-2 or other potential microfibrils. LTBP-2 thus actively regulates the differential usage of microfibrils in elastic fiber assembly.

presence of LTBP-2, and that downregulation of LTBP-2 causes fibrillin-1-independent deposition of DANCE and elastin on fibrillin-2 or other potential microfibrils. Moreover, recombinant LTBP-2 promotes deposition of DANCE on fibrillin-1 microfibrils. We propose that LTBP-2 might function as a molecular switch that determines which microfibrils DANCE should be deposited on, thereby regulating subsequent assembly of elastic fiber components. Further studies will be required to elucidate the role of LTBP-2 in elastic fiber assembly *in vivo* and the mechanism of the regulation of DANCE targeting.

Materials and methods

Cell culture

293T cells, bovine aortic smooth muscle cells (ASMCs), and human skin fibroblasts (HSFs) were maintained in DMEM (Sigma) supplemented with 2 mM glutamine, 10% penicillin/streptomycin, and 10% FBS at 37°C in 5% CO_2. HSFs, which were taken from the facial skin of 3-month-old baby, were kindly provided by Dr M Naito (Kyoto University). These HSFs were passed for 8 to 10 times before following experiments.

Metabolic labeling and immunoprecipitation

The culture medium of bovine ASMCs was changed to Cys/Met-free DMEM (Invitrogen) supplemented with 0.5 mCi. of ^{35}S-Cys/Met (Amersham) and 10% FBS, and the cultures were incubated overnight. An aliquot (5 ml) of the conditioned media was mixed with 20 μg of purified FLAG-tagged DANCE protein, and subjected to immunoprecipitation with anti-FLAG M2 affinity gel (Sigma). Other aliquots, 1.6 ml each, were subjected to immunoprecipitation with the following antibodies conjugated with protein-G/A Sepharose (Amersham): anti-human elastin monoclonal (Chemicon), anti-bovine tropoelastin monoclonal (Elastin Products Company (EPC), MM436), anti-human fibrillin-1 polyclonal (EPC, PR684), anti-human fibrillin-1 monoclonal (Neo Marker), anti-human fibrillin-2 polyclonal (EPC, PR225), or anti-bovine LTBP-2 monoclonal (EPC, MM425). Immune complexes were resolved by SDS–PAGE. The SDS–polyacrylamide gel was dried, and exposed to X-ray film.

Plasmid construction

Human full-length DANCE cDNA was cloned as described previously (Nakamura *et al*, 1999). pEF6/V5 (Invitrogen) was modified by incorporation of a C-terminal FLAG-tag or Myc-tag (pEF6/FLAG, pEF6/Myc). The DANCE ΔN1- (Δnucleotide(nt) 247-399) and ΔN2- (Δnt 247-504) DANCE cDNAs were amplified by PCR, and subcloned into pEF6/FLAG. ΔM1- (Δexon 5), ΔM2- (Δexon 6), ΔM3- (Δexon 7), ΔM4- (Δexon 8), ΔM5- (Δexon 9), ΔC1- (Δexons 10 and 11), and ΔC2-DANCE (Δexon 10) cDNA fragments were amplified by inverse PCR, followed by self-ligation. Human DANCE cDNA sequences are numbered according to GenBank™ accession number AF112152.

An expression vector encoding human full-length LTBP-2 was kindly provided by Dr J Keski-Oja (University of Helsinki). To prepare the FLAG-tagged LTBP-2 mutants, pEF6/V5 was modified by incorporation of an N-terminal FLAG-tag, following the preprotrypsin signal sequence (accatgtctgcacttctgatcctagctcttgttg gagctgcagttgct) (pEF6/ssFLAG). The following fragments of LTBP-2 cDNA were amplified by PCR, and subcloned into pEF6/ssFLAG: LTBP-2-A (exons 1–5), -B (exons 6–15), -C (exons 16–22), -D (exons 23–28), -E (exons 29–36), -F (exons 1–3), -G (exons 4–6), -H (exon 4), and -I (exon 5). LTBP-2-G-Ig, -H-Ig, and -I-Ig were C-terminal fusion proteins with the Fc portion of human IgG (nt 759–1457). Human LTBP-2 and Ig Fc portion cDNA sequences were obtained from GenBank accession number S82451 and Y14735, respectively. The coding region of each molecule was subcloned into pEF6/Myc. All constructs were confirmed by sequencing (ABI Prism 3100).

Transfection, in vitro binding assay, and Western blotting

293T cells were transfected using LipofectAMINE PLUS (Invitrogen). After transfection, they were cultured in serum-free DMEM/F12 (Sigma). The mixtures of conditioned media and cell lysates were subjected to immunoprecipitation with anti-FLAG M2 affinity gel followed by Western blotting as described previously (Hirai *et al*, 2007).

In situ Hybridization

We fixed neonatal mouse tissues in 4% PFA and embedded them in histoparaffin (Wako). The DANCE and LTBP-2 riboprobes were prepared as described previously (Shipley *et al*, 2000). Synthesis of *in situ* hybridization probes was carried out using the Riboprobe *in vitro* Transcription Systems (Promega). Paraffin sections were subjected to *in situ* hybridization as described previously (Nakamura *et al*, 1999). Counterstaining was performed with 0.02% toluidine blue. Samples were observed with an Axioplan 2 microscope (Zeiss) using a × 5 objective. Pictures were taken with an AxioCam HR digital camera (Zeiss) and AxioVision 3.1 software (Zeiss).

Mouse tissue extraction

Lung tissue samples were homogenized in PBS using a Polytron homogenizer (PT10-35, Kinematica AG). After centrifugation, the supernatants were subjected to immunoprecipitation with an anti-mouse DANCE polyclonal antibody (BSYN2473), followed by

Western blotting. Either anti-mouse LTBP-2 polyclonal or anti-mouse DANCE polyclonal antibody was used as a primary antibody. HRP-conjugated anti-rabbit polyclonal antibody (Santa Cruz) or rabbit IgG TrueBlot™ (eBioscience), respectively, was used as a secondary antibody. Anti-DANCE antibody (BSYN2473) was generated by BioSynthesis Inc. as described previously (Yanagisawa *et al*, 2002). Anti-LTBP-2 antibodies were raised by Sigma Aldrich Japan against KLH-conjugated polypeptides, CEVIPEEEFDPQNAR and CASDLEEYDAEEGH, which correspond respectively to amino acids 234–247 and 1384–1397 of mouse LTBP-2 protein.

Expression and purification of DANCE and LTBP-2 proteins

Human DANCE and LTBP-2 cDNAs were subcloned into pEF6/FLAG-His to add C-terminal His_6 and FLAG-tag. Recombinant proteins were purified, qualified, and quantified as described previously (McLaughlin *et al*, 2006).

BIAcore analysis

For kinetic binding studies, Biacore X was used. Purified recombinant DANCE protein was immobilized onto CM5 sensor chips by amine coupling in 10 mM sodium acetate (pH 4.0), giving 765.7 Response Units (RU). Subsequent binding experiments were performed in HBS-P buffer (BIACORE). The sensor chip was regenerated in 10 mM glycine-HCl, pH 2.0. Dissociation constants (K_D) were determined by fitting all curves at once with the 1:1 Langmuir binding model using BIAevaluation software.

Gene knockdown experiments and reverse transfection

Duplexed RNA oligonucleotides (Stealth™ Select RNAi) were designed using BLOCK-iT™ RNAi Designer, and synthesized by Invitrogen. Three different sequences of RNAi duplexes were synthesized for each target gene and mixed for use to minimize off-target effects. Mixed RNAi duplexes (at final concentration 15 nM) were reverse transfected into HSFs using Lipofectamine 2000 (Invitrogen). Sequence information for the Stealth™ Select RNAi duplexes is provided in Supplementary Table I).

Reverse transcription–polymerase chain reaction and quantitative PCR

Total RNAs were extracted and transcribed to cDNA followed by qPCR as described previously (Hirai *et al*, 2007). Primers used for qPCR are provided in Supplementary Table II.

Immunocytochemical staining

HSFs were cultured on microscope cover glasses (Fisherbrand). The cells were fixed with 100% methanol at −20°C. The primary antibodies used were anti-human elastin polyclonal (PR533, EPC), anti-human DANCE monoclonal (10A), anti-human fibrillin-1 polyclonal (PR217, EPC), and anti-human fibrillin-2 monoclonal (mAb143) antibodies. The secondary antibodies used were Alexa 488, 546, or 647 anti-rabbit or mouse IgG (Invitrogen), followed by nuclear staining with Hoechst 33258. Stained cells were mounted with ProLong Gold antifade reagent (Invitrogen), and visualized using an Olympus confocal microscope (FV1000). Pictures were taken with FV10-ASW 1.4 software (Olympus). Anti-DANCE antibody (10A) was raised by Iwaki & Co Ltd, Japan by immunization of DANCE null mice with purified recombinant human DANCE protein. Anti-fibrillin-2 antibody (mAb143) was generously provided by Dr Lynn Y. Sakai (Shriners Hospital for Children, Oregon Health and Science University).

Solid phase binding assay

Various concentrations of recombinant FLAG-tagged LTBP-2 or DANCE were used as soluble ligands. Solid phase binding assays using purified tropoelastin were performed as described previously with the modification of 2 mM $CaCl_2$ added in the reaction buffer (McLaughlin *et al*, 2006). The primary antibody used was anti-FLAG M2 antibody (Sigma). The secondary antibody used was HRP-conjugated anti-mouse IgG antibody (Santa Cruz). Signals were detected with Substrate Reagent Pack (R&D).

Supplementary data

Supplementary data are available at *The EMBO Journal* Online (http://www.embojournal.org).

Acknowledgements

We thank Ms N Tomikawa for excellent technical assistance. This work was supported in part by Japan Health and Labour Sciences Research Grants, Japan Society for the Promotion of Science, Japan Science and Technology Agency, Takeda Science Foundation, Sakakibara Memorial Foundation, and Japan Heart Foundation Research Grants to TN, by grants from the Ministry of Education, Science and Culture of Japan to TN and TK, and by grants from the Japan Society for the Promotion of Science, Japan Heart Foundation Research grant on Arteriosclerosis *Update* to MH.

References

Arteaga-Solis E, Gayraud B, Lee SY, Shum L, Sakai L, Ramirez F (2001) Regulation of limb patterning by extracellular microfibrils. *J Cell Biol* **154:** 275–281

Bailey AJ (2001) Molecular mechanisms of ageing in connective tissues. *Mech Ageing Dev* **122:** 735–755

Carta L, Pereira L, Arteaga-Solis E, Lee-Arteaga SY, Lenart B, Starcher B, Merkel CA, Sukoyan M, Kerkis A, Hazeki N, Keene DR, Sakai LY, Ramirez F (2006) Fibrillins 1 and 2 perform partially overlapping functions during aortic development. *J Biol Chem* **281:** 8016–8023

Charbonneau NL, Dzamba BJ, Ono RN, Keene DR, Corson GM, Reinhardt DP, Sakai LY (2003) Fibrillins can co-assemble in fibrils, but fibrillin fibril composition displays cell-specific differences. *J Biol Chem* **278:** 2740–2749

Chaudhry SS, Gazzard J, Baldock C, Dixon J, Rock MJ, Skinner GC, Steel KP, Kielty CM, Dixon MJ (2001) Mutation of the gene encoding fibrillin-2 results in syndactyly in mice. *Hum Mol Genet* **10:** 835–843

Freeman LJ, Lomas A, Hodson N, Sherratt MJ, Mellody KT, Weiss AS, Shuttleworth A, Kielty CM (2005) Fibulin-5 interacts with fibrillin-1 molecules and microfibrils. *Biochem J* **388:** 1–5

Gibson MA, Hatzinikolas G, Davis EC, Baker E, Sutherland GR, Mecham RP (1995) Bovine latent transforming growth factor beta 1-binding protein 2: molecular cloning, identification of tissue isoforms, and immunolocalization to elastin-associated microfibrils. *Mol Cell Biol* **15:** 6932–6942

Gibson MA, Hatzinikolas G, Kumaratilake JS, Sandberg LB, Nicholl JK, Sutherland GR, Cleary EG (1996) Further characterization of proteins associated with elastic fiber microfibrils including the molecular cloning of MAGP-2 (MP25). *J Biol Chem* **271:** 1096–1103

Gibson MA, Hughes JL, Fanning JC, Cleary EG (1986) The major antigen of elastin-associated microfibrils is a 31-kDa glycoprotein. *J Biol Chem* **261:** 11429–11436

Giltay R, Kostka G, Timpl R (1997) Sequence and expression of a novel member (LTBP-4) of the family of latent transforming growth factor-beta binding proteins. *FEBS Lett* **411:** 164–168

Hirai M, Ohbayashi T, Horiguchi M, Okawa K, Hagiwara A, Chien KR, Kita T, Nakamura T (2007) Fibulin-5/DANCE has an elastogenic organizer activity that is abrogated by proteolytic cleavage *in vivo*. *J Cell Biol* **176:** 1061–1071

Hirani R, Hanssen E, Gibson MA (2007) LTBP-2 specifically interacts with the amino-terminal region of fibrillin-1 and competes with LTBP-1 for binding to this microfibrillar protein. *Matrix Biol* **26:** 213–223

Hyytiainen M, Penttinen C, Keski-Oja J (2004) Latent TGF-beta binding proteins: extracellular matrix association and roles in TGF-beta activation. *Crit Rev Clin Lab Sci* **41:** 233–264

Hyytiäinen M, Taipale J, Heldin CH, Keski-Oja J (1998) Recombinant latent transforming growth factor beta-binding protein 2 assembles to fibroblast extracellular matrix and is susceptible to proteolytic processing and release. *J Biol Chem* **273:** 20669–20676

Kanzaki T, Olofsson A, Moren A, Wernstedt C, Hellman U, Miyazono K, Claesson-Welsh L, Heldin CH (1990) TGF-beta 1 binding protein: a component of the large latent complex of TGF-beta 1 with multiple repeat sequences. *Cell* **61:** 1051–1061

Kapetanopoulos A, Fresser F, Millonig G, Shaul Y, Baier G, Utermann G (2002) Direct interaction of the extracellular matrix protein DANCE with apolipoprotein(a) mediated by the kringle IV-type 2 domain. *Mol Genet Genomics* **267:** 440–446

Liu X, Zhao Y, Gao J, Pawlyk B, Starcher B, Spencer JA, Yanagisawa H, Zuo J, Li T (2004) Elastic fiber homeostasis requires lysyl oxidase-like 1 protein. *Nat Genet* **36:** 178–182

Mariencheck MC, Davis EC, Zhang H, Ramirez F, Rosenbloom J, Gibson MA, Parks WC, Mecham RP (1995) Fibrillin-1 and fibrillin-2 show temporal and tissue-specific regulation of expression in developing elastic tissues. *Connect Tissue Res* **31:** 87–97

McLaughlin PJ, Chen Q, Horiguchi M, Starcher BC, Stanton JB, Broekelmann TJ, Marmorstein AD, McKay B, Mecham R, Nakamura T, Marmorstein LY (2006) Targeted disruption of fibulin-4 abolishes elastogenesis and causes perinatal lethality in mice. *Mol Cell Biol* **26:** 1700–1709

Moren A, Olofsson A, Stenman G, Sahlin P, Kanzaki T, Claesson-Welsh L, ten Dijke P, Miyazono K, Heldin CH (1994) Identification and characterization of LTBP-2, a novel latent transforming growth factor-beta-binding protein. *J Biol Chem* **269:** 32469–32478

Nakamura T, Lozano PR, Ikeda Y, Iwanaga Y, Hinek A, Minamisawa S, Cheng CF, Kobuke K, Dalton N, Takada Y, Tashiro K, Ross Jr J, Honjo T, Chien KR (2002) Fibulin-5/DANCE is essential for elastogenesis *in vivo*. *Nature* **415:** 171–175

Nakamura T, Ruiz-Lozano P, Lindner V, Yabe D, Taniwaki M, Furukawa Y, Kobuke K, Tashiro K, Lu Z, Andon NL, Schaub R, Matsumori A, Sasayama S, Chien KR, Honjo T (1999) DANCE, a novel secreted RGD protein expressed in developing, atherosclerotic, and balloon-injured arteries. *J Biol Chem* **274:** 22476–22483

Nguyen AD, Itoh S, Jeney V, Yanagisawa H, Fujimoto M, Ushio-Fukai M, Fukai T (2004) Fibulin-5 is a novel binding protein for extracellular superoxide dismutase. *Circ Res* **95:** 1067–1074

Nunes I, Gleizes PE, Metz CN, Rifkin DB (1997) Latent transforming growth factor-beta binding protein domains involved in activation and transglutaminase-dependent cross-linking of latent transforming growth factor-beta. *J Cell Biol* **136:** 1151–1163

Pasquali-Ronchetti I, Baccarani-Contri M (1997) Elastic fiber during development and aging. *Microsc Res Tech* **38:** 428–435

Pereira L, Andrikopoulos K, Tian J, Lee SY, Keene DR, Ono R, Reinhardt DP, Sakai LY, Biery NJ, Bunton T, Dietz HC, Ramirez F (1997) Targetting of the gene encoding fibrillin-1 recapitulates the vascular aspect of Marfan syndrome. *Nat Genet* **17:** 218–222

Ramirez F, Sakai LY, Dietz HC, Rifkin DB (2004) Fibrillin microfibrils: multipurpose extracellular networks in organismal physiology. *Physiol Genomics* **19:** 151–154

Rosenbloom J, Abrams WR, Mecham R (1993) Extracellular matrix 4: the elastic fiber. *FASEB J* **7:** 1208–1218

Saharinen J, Keski-Oja J (2000) Specific sequence motif of 8-Cys repeats of TGF-beta binding proteins, LTBPs, creates a hydrophobic interaction surface for binding of small latent TGF-beta. *Mol Biol Cell* **11:** 2691–2704

Saharinen J, Taipale J, Monni O, Keski-Oja J (1998) Identification and characterization of a new latent transforming growth factor-beta-binding protein, LTBP-4. *J Biol Chem* **273:** 18459–18469

Sakai LY, Keene DR, Engvall E (1986) Fibrillin, a new 350-kD glycoprotein, is a component of extracellular microfibrils. *J Cell Biol* **103:** 2499–2509

Shipley JM, Mecham RP, Maus E, Bonadio J, Rosenbloom J, McCarthy RT, Baumann ML, Frankfater C, Segade F, Shapiro SD (2000) Developmental expression of latent transforming growth factor beta binding protein 2 and its requirement early in mouse development. *Mol Cell Biol* **20:** 4879–4887

Taipale J, Lohi J, Saarinen J, Kovanen PT, Keski-Oja J (1995) Human mast cell chymase and leukocyte elastase release latent transforming growth factor-beta 1 from the extracellular matrix of cultured human epithelial and endothelial cells. *J Biol Chem* **270:** 4689–4696

Yanagisawa H, Davis EC, Starcher BC, Ouchi T, Yanagisawa M, Richardson JA, Olson EN (2002) Fibulin-5 is an elastin-binding protein essential for elastic fibre development *in vivo*. *Nature* **415:** 168–171

Yin W, Smiley E, Germiller J, Mecham RP, Florer JB, Wenstrup RJ, Bonadio J (1995) Isolation of a novel latent transforming growth factor-beta binding protein gene (LTBP-3). *J Biol Chem* **270:** 10147–10160

Zanetti M, Braghetta P, Sabatelli P, Mura I, Doliana R, Colombatti A, Volpin D, Bonaldo P, Bressan GM (2004) EMILIN-1 deficiency induces elastogenesis and vascular cell defects. *Mol Cell Biol* **24:** 638–650

Zhang H, Apfelroth SD, Hu W, Davis EC, Sanguineti C, Bonadio J, Mecham RP, Ramirez F (1994) Structure and expression of fibrillin-2, a novel microfibrillar component preferentially located in elastic matrices. *J Cell Biol* **124:** 855–863

Zhang H, Hu W, Ramirez F (1995) Developmental expression of fibrillin genes suggests heterogeneity of extracellular microfibrils. *J Cell Biol* **129:** 1165–1176

Original Article

Polymorphisms of Apolipoprotein E and Methylenetetrahydrofolate Reductase in the Japanese Population

Hidenori Arai[1], Akira Yamamoto[2], Yuji Matsuzawa[3], Yasushi Saito[4], Nobuhiro Yamada[5], Shinichi Oikawa[6], Hiroshi Mabuchi[7], Tamio Teramoto[8], Jun Sasaki[9], Noriaki Nakaya[10], Hiroshige Itakura[11], Yuichi Ishikawa[12], Yasuyoshi Ouchi[13], Hiroshi Horibe[14], Tohru Egashira[15], Hiroaki Hattori[15], and Toru Kita[16]

[1]Department of Geriatric Medicine, Kyoto University Graduate School of Medicine, Japan.
[2]National Cardiovascular Center, Japan.
[3]Sumitomo Hospital, Japan.
[4]Department of Clinical Cell Biology and Medicine, Chiba University, Japan.
[5]Department of Internal Medicine, University of Tsukuba, Japan.
[6]Department of Internal Medicine, Nippon Medical School, Japan.
[7]Department of Laboratory Science, Kanazawa University, Japan.
[8]Department of Internal Medicine, Teikyo University, Japan.
[9]International University of Health and Welfare, Japan.
[10]Fussa Hospital, Japan.
[11]Ibaraki Christian University, Japan.
[12]Faculty of Health Sciences, Kobe University, Japan.
[13]Department of Geriatric Medicine, University of Tokyo, Japan.
[14]Keisen Clinic, Japan.
[15]Department of Advanced Technology and Development, BML, Inc., Japan.
[16]Department of Cardiovascular Medicine, Kyoto University Graduate School of Medicine, Japan.

Aim: The aim of this study is to analyze the effect of apolipoprotein E (apo E) and methylenetetrahydrofolate reductase (*MTHFR*) gene polymorphisms on serum lipid and homocysteine levels in the general Japanese population.
Methods: We analyzed the polymorphisms in individuals randomly selected from among participants of Serum Lipid Survey 2000.
Results: The frequency of the ε2, ε3, and ε4 alleles of *APOE* was 4.2, 85.3, and 10.5%, respectively. Individuals with the genotype ε4/ε4 had the highest total and low-density lipoprotein (LDL) cholesterol levels, while those with ε2/ε2 had the lowest. Individuals with the ε2/ε2 and ε2/ε4 genotypes had higher remnant-like particles (RLP)-cholesterol levels than those with ε2ε3, ε3ε3, and ε3ε4. There was a trend for individuals with the ε2/ε4 and ε2/ε2 genotypes to have higher triglyceride levels, although the difference was not significant. The presence of the T allele in a *MTHFR* polymorphism (C667T) was associated with higher homocysteine levels, which is more prominent in men than in women.
Conclusion: Thus in our large-scale analysis we have shown that RLP-cholesterol is better associated with *APOE* genotype than triglyceride and the effect of the T allele on *MTHFR* polymorphism (C667T) homocysteine levels is more prominent in men than in women among Japanese.

J Atheroscler Thromb, 2007; 14:167-171.

Key words; Hyperlipidemia, Polymorphism, Apolipoprotein E, *MTHFR*, Homocysteine

Address for correspondence: Hidenori Arai, Department of Geriatric Medicine, Kyoto University School of Medicine, 54 Kawahara-cho, Shogoin, Sakyo-ku, Kyoto 606-8507, Japan.
E-mail: harai@kuhp.kyoto-u.ac.jp
Received: January 22, 2007
Accepted for publication: March 14, 2007

Introduction

Apolipoprotein E (apo E) is an important structural constituent of serum chylomicrons, very low-density lipoproteins, and high-density lipoproteins (HDL) and plays a critical role in lipoprotein metablism, where it can facilitate the clearance of remnant lipoprotein and cellular efflux of cholesterol[1]. Apo E has three polymorphisms, ε2, ε3, and ε4, which affect lipoprotein metabolism and atherosclerosis[2]. The ε4 allele is associated with higher low-density lipoprotein (LDL) cholesterol levels than the other alleles and with a higher incidence of coronary heart disease[3]. Apo E4 is also shown to be involved in the development of Alzheimer's disease[4], while homozygosity for apo E2 is associated with the development of type Ⅲ hyperlipidemia[5].

We also studied the *MTHFR* gene because its polymorphisms affect serum homocysteine levels and homocysteine is also associated with cardiovascular disease and Alzheimer's disease[6-9]. An elevated homocysteine level is associated with coronary heart disease and the C677T polymorphism in the *MTHFR* gene results in reduced *MTHFR* enzyme activity and reduced methylation of homocysteine to methioneine resulting in mild hyperhomocysteinemia[10]. Although several studies have examined the incidence of *APOE* and *MTHFR* polymorphisms[8, 11], these has been no large-scale study to determine the incidence of *APOE* and *MTHFR* polymorphisms and their association with lipoprotein profiles and homocysteine levels in the general Japanese population. In 2000, we conducted a lipid survey in the Japanese population, 12,839 people all over the country. In this survey, we examined *APOE* and *MTHFR* gene polymorphisms to determine the incidence of each and its relationship with lipid profiles and homocysteine levels in the Japanese.

Methods

Design and Data Collection

This work is part of Serum Lipid Level Survey 2000 from various parts of Japan. The Ethics committee, Graduate School and Faculty of Medicine, Kyoto University approved the study protocol and all subjects provided written informed consent for participation in the gene analysis. The handling of DNA samples followed the guidelines from the Ministry of Health, Labor, and Welfare. In Serum Lipid Survey 2000, a total of 12,839 subjects were recruited at 36 hospitals across the country. The subjects in the present study were participants in the survey at 9 hospitals from whom informed content for genotyping was sought. Of the 12,839 subjects, 2,267 (17.7%) with no lipid-altering medication were randomly selected for the present study. Among the 2,267 participants, we examined serum homocysteine levels and *MTHFR* gene polymorphisms in 505 participants.

Laboratory Methods

All serum and blood samples were obtained in the fasting state. All lipid and other analyses were conducted on venous blood samples within one week of collection at BML (Saitama, Japan). Serum cholesterol and TG levels were measured by enzymatic assay. HDL-cholesterol and LDL-cholesterol levels were measured enzymatically with a kit from Daiichi Kagaku Co. Ltd. (Tokyo, Japan). The results of lipid analyses in the four surveys were indirectly standardized according to the criteria of the CDC Lipid Standardization Program[12]. The serum homocysteine level was assayed by high performance liquid chromatography with fluorescent detection as described by Ubbink *et al.*[13]. DNA was extracted with a QIAamp DNA blood kit (Qiagen, Hilden, Germany).

Detection of gene Mutations by Invader® Assay

We used the Invader® assay to screen for mutations of the *APOE* and *MTHFR* genes, as previously described. In brief, the probe/Invader®/MgCl2 mixture was prepared by combining 3 μL of primary probe/Invader® mix and 5 μL of 22.5 mM MgCl2 per reaction. The primary probes/Invader® mixture contained 3.5 μmol/L wild primary probe, 3.5 μmol/L mutant primary probe, 0.35 μmol/L Invader® oligonucleotide, and 10 mmol/L MOPS. Eight microliters of primary probe/Invader®/MgCl2 mixture was added per well of a 96-well plate. Seven microliters of 5 fmol/L synthetic target oligonucleotides, 10 μg/mL yeast tRNA (no target blank), and genomic DNA (15 ng/μL) were added, and denatured by incubation at 95℃ for 10 min. After 15 μL of mineral oil (Sigma, St. Louis, MO) was overlayed into all reaction wells, the plate was incubated isothermally at 63℃ for 4 h in a DNA thermalcycler (PTC-200; MJ Research, Watertown, MA) and then kept at 4℃ until fluorescence were measured. The intensity of the fluorescence was measured with a fluorescence microtiter plate reader (Cytoflour 4000; Applied Biosystems) with excitation at 485 nm/20 nm (Wavelength/Bandwidth) and emission at 530 nm/25 nm for FAM; and excitation at 560 nm/20 nm and emission at 620 nm/40 nm for RED. The genotyping was analyzed by calculating the ratio of net counts with wild primary probe to net counts with mutant primary probe. The probes used in this study were designed and synthesized by Third Wave Technologies, Inc (Madison, WI).

Data Analyses

Differences in means were evaluated with an analysis of variance. The analysis was performed with the statistical Package for Social Sciences (SPSS Japan Inc. ver. 11.5, Tokyo, Japan).

Results

We investigated the frequency and phenotypic association of *APOE* gene polymorphisms of 2,267 subjects. We found that the SNPs were in Hardy-Weinberg equilibrium. As previously described, the mean age, total cholesterol, TG, HDL-cholesterol, and LDL-cholesterol levels in this population were similar to the levels for all 12,839 patients in Serum Lipid Survey 2000[14]. We also found that the medians of total, LDL-, and HDL-cholesterol levels did not differ appreciably from the means, thereby excluding gross right-hand tailing of the distribution (data not shown). These data indicate that the participants in the gene analysis are representative of the general Japanese population.

The genotype and allelic frequency of *APOE* polymorphisms are presented in **Table 1**. The frequency of the ε2, ε3, and ε4 alleles was 4.2, 85.3, and 10.5%, respectively. As in other studies, the genotypes ε2ε2, ε2ε4, and ε4ε4 were quite rare. High frequencies of the ε3 allele are also found in Chinese, but the frequency is lower in Caucasians[15].

Table 1. Genotype and allele frequency of *APOE* gene in Japanese.

genotype	*n*	%	alleles	*n*	%
ε2/ε2	9	0.4	ε2	192	4.2
ε2/ε3	155	6.8	ε3	3,868	85.3
ε2/ε4	19	0.8	ε4	474	10.5
ε3/ε3	1,653	72.9			
ε3/ε4	407	18.0			
ε4/ε4	24	1.1			

We next examined the association of the *APOE* genotype and lipid profiles in these participants. As shown in **Table 2**, all the lipid parameters and blood glucose differed significantly among these genotypes by ANOVA. Total cholesterol, triglyceride, HDL-cholesterol, LDL-cholesterol, and RLP-cholesterol levels were different among the groups. The *p* values are shown in the right column. According to the post-hoc analysis, the total cholesterol level was significantly lower for genotype ε2ε2 than ε4ε4 and genotype ε2ε3 than ε3ε3, ε2ε4, or ε4ε4. The HDL-cholesterol level was significantly higher for ε2ε3 than ε2ε4. The LDL-cholesterol level was significantly lower for genotypes ε2ε2 and ε2ε3 than for ε3ε3, ε3ε4, and ε4ε4. The RLP-cholesterol level was significantly higher for ε2ε2 than ε2ε3, ε3ε3, ε3ε4, or ε4ε4 and for genotype ε2ε4 than ε2ε3, ε3ε3, or ε3ε4, although there was no significant difference in triglyceride levels according to the post-hoc analysis. Blood glucose or age did not differ significantly among the groups.

We next examined the association of the *MTHFR* C667T polymorphism with serum homocysteine levels in 505 samples randomly selected from 2,267 samples. As shown in **Table 3**, the incidence of the CC, CT, and TT genotypes was 33.9, 46.1, and 20.0%, respectively. The TT genotype was significantly associated with higher homocysteine levels in men and women, and statistical significance was found between CC and TT and between CT and TT by a post-hoc analysis. However, the difference was more prominent in men.

Discussion

There, we have shown in a large-scale study, the

Table 2. Mean of serum lipid levels and blood glucose in each genotype of *APOE* in Japanese.

	ε2/ε2	ε2/ε3	ε2/ε4	ε3/ε3	ε3/ε4	ε4/ε4	total	*p* value
	mean ± SEM	mean ± SEM	mean ± SEM	mean ± SEM	mean ± SEM	mean ± SEM	mean ± SEM	
T-cho	165.0 ± 23.8	189.7 ± 3.00	202.9 ± 12.6	201.8 ± 0.92	206.8 ± 1.95	223.3 ± 9.18	202.1 ± 0.81	<0.0001
TG	171.4 ± 52.8	118.8 ± 8.55	189.0 ± 53.3	117.0 ± 2.41	128.0 ± 5.16	127.9 ± 18.9	119.8 ± 2.13	0.023
HDL-c	51.2 ± 9.51	63.6 ± 1.92	53.0 ± 3.07	59.8 ± 0.41	58.0 ± 0.82	61.9 ± 3.48	59.7 ± 0.36	0.007
LDL-c	70.5 ± 5.63	101.9 ± 2.75	117.2 ± 8.07	118.5 ± 0.91	120.5 ± 1.93	131.5 ± 7.97	117.7 ± 0.79	<0.0001
RLP-c	22.9 ± 1.15	4.4 ± 0.37	12.5 ± 7.59	4.7 ± 0.17	5.2 ± 0.33	4.1 ± 0.58	4.8 ± 0.15	<0.0001
FBS	121.3 ± 19.5	104.7 ± 3.27	110.6 ± 9.37	103.9 ± 0.94	103.3 ± 2.17	88.6 ± 2.54	103.9 ± 0.83	0.461
age	52.8 ± 10.1	49.5 ± 2.11	50.8 ± 53.2	46.7 ± 0.69	47.4 ± 1.30	43.2 ± 4.61	47.1 ± 0.58	0.659

T-cho: total cholesterol (mg/dL), TG: triglyceride (mg/dL), HDL-c: HDL-cholesterol (mg/dL), LDL-c: LDL-cholesterol (mg/dL), RLP-c: remnant-like particles cholesterol (mg/dL), FBS: fasting blood sugar (mg/dL), SEM: standard error of the mean

Table 3. Genotype frequency of the *MTHFR* gene and its association with serum homocysteine levels in Japanese.

total					
genotype	*n*	%	mean	SEM	
CC	171	33.9	10.9	0.3	$p<0.001$
CT	233	46.1	11.6	0.24	
TT	101	20.0	15.7	1.23	
total	505	100	12.2	0.29	
male					
genotype	*n*	%	mean	SEM	
CC	92	33.6	10.7	0.36	$p<0.001$
CT	132	48.2	12.9	0.35	
TT	50	18.2	19.8	2.41	
total	274	100	13.4	0.52	
female					
genotype	*n*	%	mean	SEM	
CC	79	34.2	10.2	0.43	$p=0.005$
CT	101	43.7	10.1	0.27	
TT	51	22.1	11.9	0.57	
total	231	100	10.5	0.23	

SEM: standard error of the mean

frequency of the *APOE* genotype in the Japanese and its association with serum lipid levels. Frequencies of *APOE* genotypes are highly heterogenous among various populations. Epidemiological data indicate that the frequency of the $\varepsilon 3$ allele is higher in Japanese and Chinese than in Caucasians, while the frequency of the $\varepsilon 4$ allele is lower in Asians than Caucasians[3, 16]. Our data indicate that the frequency of the $\varepsilon 3$ allele is quite consistent with previous reports in Japanese[8, 11, 16, 17], and is slightly higher than that of Icelandic and Hungarian populations and much higher than that in the Finnish population[15].

Our study confirmed that the $\varepsilon 4$ allele is associated with higher, and the $\varepsilon 2$ allele is associated with lower, LDL cholesterol levels. Although there was a trend for individuals with the genotypes $\varepsilon 2/\varepsilon 4$ and $\varepsilon 2/\varepsilon 2$ to have higher triglyceride levels, it was not statistically significant by a post-hoc analysis, probably because triglyceride levels are highly variable. However, individuals with $\varepsilon 2/\varepsilon 4$ and $\varepsilon 2/\varepsilon 2$ had significantly higher RLP-cholesterol levels than did those with the other genotypes, indicating that RLP-cholesterol might be better correlated with *APOE* genotype. Although in this study we could not compare the body mass index of $\varepsilon 2/\varepsilon 2$ homozygotes, it would be intriguing to know whether individuals with the $\varepsilon 2/\varepsilon 4$ and $\varepsilon 2/\varepsilon 2$ genotypes have metabolic abnormalities, such as abdominal obesity and insulin resistance, because they have higher triglyceride, RLP-cholesterol, and blood glucose levels.

Elevated levels of homocysteine have been considered a risk for cardiovascular disease. Our study is consistent with other studies that show higher homocysteine levels in people with the TT genotype. However, the relationship between the C677T *MTHFR* polymorphism and cardiovascular disease is still controversial. Because our study population is made up of healthy volunteers, a prospective study is necessary to determine which genotype is associated with cardiovascular risk.

In summary, we have provided the largest database of gene polymorphisms related to lipid metabolism and homocysteine in the general Japanese population. A prospective study is necessary to determine the contribution of these gene polymorphisms to cardiovascular risk in Japanese.

Acknowledgements

We thank Shizuya Yamashita (Osaka University) and Hideaki Bujo (Chiba University) for critical reading of the manuscript. This study was supported by research grants for health sciences from the Japanese Ministry of Health and a grant from the Japan Atherosclerosis Society. We also thank Osaka Pharmaceutical Manufactures Association for supporting our work.

References

1) Curtiss LK and Boisvert WA: Apolipoprotein E and atherosclerosis. Curr Opin Lipidol, 2000; 11:243-251
2) Davignon J, Gregg RE, and Sing CF: Apolipoprotein E polymorphism and atherosclerosis. Arteriosclerosis, 1988; 8:1-21
3) Wang XL, McCredie RM, and Wilcken DE: Polymorphisms of the apolipoprotein E gene and severity of coronary artery disease defined by angiography. Arterioscler Thromb Vasc Biol, 1995; 15:1030-1034
4) Katzman R: Apolipoprotein E and Alzheimer's disease. Curr Opin Neurobiol, 1994; 4:703-707
5) Rall SC Jr. and Mahley RW: The role of apolipoprotein E genetic variants in lipoprotein disorders. J Intern Med, 1992; 231:653-659
6) Boushey CJ, Beresford SA, Omenn GS, and Motulsky AG: A quantitative assessment of plasma homocysteine as a risk factor for vascular disease. Probable benefits of increasing folic acid intakes. JAMA, 1995; 274:1049-1057
7) Graham IM, Daly LE, Refsum HM, Robinson K, Brattstrom LE, Ueland PM, Palma-Reis RJ, Boers GH, Sheah-

an RG, Israelsson B, Uiterwaal CS, Meleady R, McMaster D, Verhoef P, Witteman J, Rubba P, Bellet H, Wautrecht JC, de Valk HW, Sales Luis AC, Parrot-Rouland FM, Tan KS, Higgins I, Garcon D, and Andria G: Plasma homocysteine as a risk factor for vascular disease. The European Concerted Action Project. Jama, 1997; 277:1775-1781

8) Ou T, Yamakawa-Kobayashi K, Arinami T, Amemiya H, Fujiwara H, Kawata K, Saito M, Kikuchi S, Noguchi Y, Sugishita Y, and Hamaguchi H: Methylenetetrahydrofolate reductase and apolipoprotein E polymorphisms are independent risk factors for coronary heart disease in Japanese: a case-control study. Atherosclerosis, 1998; 137:23-28
9) Clarke R, Smith AD, Jobst KA, Refsum H, Sutton L, and Ueland PM: Folate, vitamin B12, and serum total homocysteine levels in confirmed Alzheimer disease. Arch Neurol, 1998; 55:1449-1455
10) Brattstrom L, Wilcken DE, Ohrvik J, and Brudin L: Common methylenetetrahydrofolate reductase gene mutation leads to hyperhomocysteinemia but not to vascular disease: the result of a meta-analysis. Circulation, 1998; 98:2520-2526
11) Shinomiya S, Sasaki J, Kiyohara C, Tsuji E, Inoue H, Marugame T, Handa K, Hayabuchi H, Hamada H, Eguchi H, Fukushima Y, and Kono S: Apolipoprotein E genotype, serum lipids, and colorectal adenomas in Japanese men. Cancer Lett, 2001; 164:33-40
12) Johnson CL, Rifkind BM, Sempos CT, Carroll MD, Bachorik PS, Briefel RR, Gordon DJ, Burt VL, Brown CD, Lippel K, and Cleeman JI: Declining serum total cholesterol levels among US adults. The National Health and Nutrition Examination Surveys. Jama, 1993; 269:3002-3008
13) Ubbink JB, Hayward Vermaak WJ, and Bissbort S: Rapid high-performance liquid chromatographic assay for total homocysteine levels in human serum. J Chromatogr, 1991; 565:441-446
14) Arai H, Yamamoto A, Matsuzawa Y, Saito Y, Yamada N, Oikawa S, Mabuchi H, Teramoto T, Sasaki J, Nakaya N, Itakura H, Ishikawa Y, Ouchi Y, Horibe H, Egashira T, Hattori H, Shirahashi N, and Kita T: Polymorphisms in four genes related to triglyceride and HDL-cholesterol levels in the general Japanese population in 2000. J Atheroscler Thromb, 2005; 12:240-250
15) Hallman DM, Boerwinkle E, Saha N, Sandholzer C, Menzel HJ, Csazar A, and Utermann G: The apolipoprotein E polymorphism: a comparison of allele frequencies and effects in nine populations. Am J Hum Genet, 1991; 49:338-349
16) Eto M, Watanabe K, and Ishii K: Reciprocal effects of apolipoprotein E alleles (epsilon 2 and epsilon 4) on plasma lipid levels in normolipidemic subjects. Clin Genet, 1986; 29:477-484
17) Kobori S, Nakamura N, Uzawa H, and Shichiri M: Influence of apolipoprotein E polymorphism on plasma lipid and apolipoprotein levels, and clinical characteristics of type III hyperlipoproteinemia due to apolipoprotein E phenotype E2/2 in Japan. Atherosclerosis, 1988; 69:81-88

Available online at www.sciencedirect.com
ScienceDirect
Biochemical and Biophysical Research Communications 363 (2007) 782–787
BBRC
www.elsevier.com/locate/ybbrc

Hypercholesterolemia contributes to the development of atherosclerosis and vascular remodeling by recruiting bone marrow-derived cells in cuff-induced vascular injury

Yang Xu [a,1], Hidenori Arai [b,*], Toshinori Murayama [a,d], Toru Kita [c], Masayuki Yokode [a,d]

[a] *Department of Clinical Innovative Medicine, Kyoto University Graduate School of Medicine, 54 Kawahara-cho, Shogoin, Sakyo-ku, Kyoto 606-8507, Japan*
[b] *Department of Geriatric Medicine, Kyoto University Graduate School of Medicine, 54 Kawahara-cho, Shogoin, Sakyo-ku, Kyoto 606-8507, Japan*
[c] *Department of Cardiovascular Medicine, Kyoto University Graduate School of Medicine, 54 Kawahara-cho, Shogoin, Sakyo-ku, Kyoto 606-8507, Japan*
[d] *Translational Research Center, Kyoto University Hospital, 54 Kawahara-cho, Shogoin, Sakyo-ku, Kyoto 606-8507, Japan*

Received 8 September 2007
Available online 19 September 2007

Abstract

Recently, the role of bone marrow (BM)-derived endothelial cells and smooth muscle cells (SMCs) has been extensively studied in the pathogenesis of atherosclerosis. In this study we examined the effect of hypercholesterolemia on cuff-induced intimal thickening in LDL-receptor knockout (LDLR−/−) mice fed with a high-fat diet. We transplanted BM of green fluorescence protein (GFP)-transgenic mice to LDLR−/− mice to identify the cell lineage in the lesion. After BM transplantation mice were fed with a high-fat diet for 4 weeks and were then planted a polyethylene cuff on the right femoral artery. Two weeks after cuff placement, atherosclerotic lesions developed in the intima predominantly consisting of a massive accumulation of foam cells with a number of α smooth muscle actin (αSMA)- and GFP-positive cells. Adventitial small vessels were positive both for CD31 and GFP. Our data indicate that BM-derived cells can contribute to the development of atherosclerosis in the presence of hypercholesterolemia.

Keywords: Hypercholesterolemia; Macrophage; Smooth muscle cell; Endothelial cell; Vascular injury; Bone marrow

Arterial injury is one of the critical initiating events in the pathogenesis of various vascular diseases, such as spontaneous atherosclerosis, transplant arteriosclerosis, restenosis after percutaneous transluminal coronary angioplasty, and vein graft atherosclerosis, where the presence of hypercholesterolemia affects the development of the lesions [1,2]. Hypercholesterolemia is a major risk factor that is associated with atherosclerotic disease and can modify the structure and function of the arterial wall in a manner that is consistent with an inflammatory response. The typical fatty streak, a characteristic vascular lesion of atherosclerosis, consists of macrophages, smooth muscle cells (SMCs), and varying numbers of T-lymphocytes that are recruited to the lesion site in response to months or years of hypercholesterolemia [3–5].

Recently, the role of bone marrow (BM)-derived endothelial cells and SMCs has been extensively studied in the pathogenesis of atherosclerosis. Our previous study has shown that BM-derived cells can differentiate into macrophage, SMCs, and endothelial cells in the cuff-induced vascular remodeling lesion in C57BL/6 mice [6]. However, the lesion formation was just occurred in the adventitia in the cuffed femoral artery in that mouse model. Thus, we could not determine the role of BM-derived cells in the lesion formation in the intima after vascular injury. That study has raised a question whether hypercholesterolemia could affect the lesion formation and the mobilization of BM-derived cells after vascular injury.

* Corresponding author. Fax: +81 75 751 3463.
E-mail address: harai@kuhp.kyoto-u.ac.jp (H. Arai).
[1] Present address: Institute of Medicinal Plant Development, Chinese Academy of Medical Sciences and Peking Union Medical College, 151 Malianwa North Road, Haidian District, Beijing 100094, PR China.

0006-291X/$ - see front matter © 2007 Elsevier Inc. All rights reserved.
doi:10.1016/j.bbrc.2007.09.029

To address this question, we established a new mouse model lacking low density lipoprotein receptor gene (LDLR−/−) and ubiquitously expressing green fluorescent protein (GFP+). We have utilized a vascular injury model induced by polyethylene cuff placement around the femoral artery after BM transplantation (BMT) from LDLR−/− and GFP+ mice to LDL−/− mice and tried to answer the question how hypercholesterolemia can modify the lesion formation in cuff-induced vascular remodeling.

Materials and methods

Mice. All experimental protocols were performed in accordance with the guidelines of Kyoto University. Low density lipoprotein receptor knockout (LDLR−/−) mice with C57Bl/6 background were a generous gift from Dr. S. Ishibashi (Jichi Medical School, Tochigi, Japan). GFP transgenic mice with C57Bl/6 background were a generous gift from Dr. M. Okabe (Osaka University, Osaka, Japan). The mice were housed and bred under specific pathogen-free conditions at the animal facility, kept in a temperature-controlled facility on a 14 h light/10 h dark cycle, with free access to food and water.

To obtain the GFP+ and LDLR−/− mice for BMT, we bred GFP transgenic mice with LDLR−/− mice and screened using a portable UV checker (Model UVGL-58, USA) and PCR. After being weaned at 4 weeks of age, mice were fed a normal chow diet (CMF, containing 8.7% (wt/wt) fat and 0.063% (wt/wt) cholesterol; Oriental Yeast, Chiba, Japan) until BMT.

BMT. Twenty-two-week-old female LDLR−/− mice were subjected to total body irradiation (9 Gy) using the Gammacell 40 Exactor Irradiator (Nordion International Inc., Ottawa, Canada). BM cell suspensions were isolated by pushing the femurs from GFP+ and LDL−/− male and female mice. BM cell suspensions were prepared by passing the cells through 70 μm nylon gauze. Each irradiated recipient received 5×10^5 bone marrow cells in 0.5 ml PBS by intravenous injection into the tail vein. After the LDLR−/− mice were subjected to total body irradiation and BMT, they were switched to a high-fat diet containing 1.25% cholesterol, 7.5% (wt/wt) cocoa butter, 7.5% casein, and 0.5% (wt/wt) sodium cholate (Oriental Yeast) until the end of the experiment period. Drinking water was supplied with 0.1% hydrochloric acid. Four weeks after BMT, the recipient mice were phlebotomized and the circulating leukocytes were then checked for the expression of GFP by flow cytometry. Cuff placement was performed at least 4 weeks after BMT.

Cuff placement. The surgical procedure of cuff placement was according to the method as described. Mice were anesthetized with barbiturate complex (propylene glycol 17.9% (v/v), ethanol 8.9% (v/v), and sodium 5-ethyl-5-(1-methylbutyl) barbiturate 10.7% (v/v)). The right femoral artery was dissected from its surroundings. A non-constrictive polyethylene cuff (PE50, 0.58 mm inner diameter, 0.965 mm outer diameter, 2 mm length. Becton Dickinson Co., Sparks, NV) was placed loosely around the right femoral artery. The control left femoral artery underwent isolation from the surrounding tissues without cuff placement.

Measurement of plasma cholesterol levels. Blood samples were taken under general anesthesia from the tail vein at the time of operation and euthanization. Total plasma cholesterol concentrations were measured enzymatically using commercially available kits (TOYOBO Co., Ltd.).

Tissue preparation and immunocytochemistry. At euthanization, mice were anesthetized with barbiturate complex. Mouse thorax was opened and physiological pressure-perfusion-fixation (100 mmHg) with 4% paraformaldehyde in PBS for 10 min was performed by cardiac puncture. After the experimental period, the mice were killed and bilateral femoral arteries were harvested. The tissue was snap-frozen in O.C.T. Compound (Sakura Finetek USA, Inc. Torrance, CA). Serial cross sections (6-μm thick) were obtained throughout the entire length of the cuffed femoral artery or equivalent portion of the contralateral artery for histological analysis.

Macrophages were detected in cuff-induced vascular injury lesion by immunohistochemistry of rat monoclonal antibody, MOMA-2 (BMA Biochemicals AG, Augst, Switzerland). Subsequently, sections were incubated with goat anti-rat IgG (BD science). Finally the sections were exposed for 30 min to avidin and biotin complex (Vectastain ABC Kit, Vector Laboratories) for amplifying the signals. For fluorescence stain of macrophage, Alexa Fluor 546 goat anti-rat IgG (Molecular Probes, Netherlands) was used after the section was incubated with MOMA-2. Lipid deposition was visualized with Oil red O (Boehringer Mannheim) staining. For SMC staining, we used mouse monoclonal anti-human smooth muscle α-actin (αSMA) antibody (clone 1A4) labeled with Cy3 (Sigma, St. Louis, MO). Endothelial cells were identified by immunohistochemical staining with biotin-conjugated rat anti-mouse CD31 antibody (Southern Biotech). For CD31 staining, Tyramide Signal Amplification system (TSA Kit with HRP–streptavidin and Alexa Flour 568 tyramide. Molecular Probes, Netherlands) was employed to increase antigenicity of ECs.

Quantification of vascular remodeling lesions. Atherosclerotic-like lesions in femoral vascular remodeling were evaluated for Oil red O staining by Image-Pro Plus (Media Cybernetics), as previously described [7–9]. Eight equally spaced cross sections were used in all mice to quantify lesions. The fraction area of the lesion stained by Oil red O was calculated by dividing the whole vessel area including the lumen, intima, media, and adventitia, as previously described [8]. The mean of the fraction area was calculated and expressed as a percentage.

Statistical analysis. Data are expressed as mean ± SD and were analyzed by ANOVA with Abacus Statview software (version 5.0). A value of $P < 0.05$ was regarded as significant.

Results

Recruitment of BM-derived progenitor cells in cuff-induced vascular remodeling

We used LDLR−/− mice as the recipient and performed cuff placement to examine the role of BM-derived cells on vascular injury. To eliminate the effect of the LDL receptor in recipient mice during vascular remodeling after BMT, we generated LDLR−/− mice which transgenically express GFP as a donor. BM cells from donor mice were transplanted into lethally irradiated LDLR−/− mice before cuff placement. After 4 weeks of BMT, we confirmed the reconstitution of the hematopoietic system by checking the fluorescence of blood leukocytes by flow cytometry. We found that more than 85% of the cells were positive for GFP (data not shown), indicating that most of the leukocytes were derived from the donor BM. After 1 or 2 weeks of cuff placement, cuffed or sham-operated femoral arteries were examined under fluorescence microscopy. In the cuffed artery, most of the cells accumulating in the lesion were GFP-positive (Fig. 1A and B), suggesting that those cells were derived from the donor BM. In contrast, in the sham-operated artery, GFP-positive cells were hardly detected (Fig. 1C). Total plasma cholesterol levels in the mice fed normal chow were 285.3 ± 19.9 mg/dl (before), 287.8 ± 22.1 mg/dl (after 2 weeks), and those fed a high-fat diet . were 288.0 ± 14.0 mg/dl (before) and 2652.0 ± 102.7 mg/dl (after 2 weeks). These data indicate that the total plasma cholesterol levels were significantly increased after high-fat diet ($n = 4$, $P < 0.01$ vs. normal chow diet). Corresponding to the increased cholesterol